Published in final edited form as:
Exp Cell Res. 2006 December 10; 312(20): 4181–4204.

Cyclin G2 is a Centrosome-associated Nucleocytoplasmic Shuttling Protein that Influences Microtubule Stability and Induces a p53-dependent Cell Cycle Arrest

Aruni S. Arachchige Don[1], **Robert F. Dallapiazza**[1], **David A. Bennin**[2], **Tiffany Brake**[2], **Colleen E. Cowan**[1], and **Mary C. Horne**[1,2,*]

1 *The Department of Pharmacology, University of Iowa, Iowa City, Iowa 52242-1109*

2 *The Department of Pharmacology, University of Wisconsin, Madison, Wisconsin 53706-1532*

Abstract

Cyclin G2 is an atypical cyclin that associates with active protein phosphatase 2A. Cyclin G2 gene expression correlates with cell cycle inhibition; it is significantly upregulated in response to DNA damage and diverse growth inhibitory stimuli, but repressed by mitogenic signals. Ectopic expression of cyclin G2 promotes cell cycle arrest, cyclin dependent kinase 2 inhibition, and the formation of aberrant nuclei [1]. Here we report that endogenous cyclin G2 copurifies with centrosomes and microtubules (MT), and that ectopic G2 expression alters microtubule stability. We find exogenous and endogenous cyclin G2 present at microtubule organizing centers (MTOCs) where it colocalizes with centrosomal markers in a variety of cell lines. We previously reported that cyclin G2 forms complexes with active protein phosphatase 2A (PP2A) and colocalizes with PP2A in a detergent resistant compartment. We now show that cyclin G2 and PP2A colocalize at MTOCs in transfected cells, and that the endogenous proteins copurify with isolated centrosomes. Displacement of the endogenous centrosomal scaffolding protein AKAP450 that anchors PP2A at the centrosome, resulted in the depletion of centrosomal cyclin G2. We find that ectopic expression of cyclin G2 induces microtubule bundling and resistance to depolymerization, inhibition of polymer regrowth from MTOCs, and a p53 dependent cell cycle arrest. Furthermore, we determined that a 100 amino acid carboxy-terminal region of cyclin G2 is sufficient to both direct GFP localization to centrosomes and induce cell cycle inhibition. Colocalization of endogenous cyclin G2 with only one of two GFP-centrin tagged centrioles, the mature centriole present at microtubule foci, indicate that cyclin G2 resides primarily on the mother centriole. Copurification of cyclin G2 and PP2A subunits with microtubules and centrosomes, together with the effects of ectopic cyclin G2 on cell cycle progression, nuclear morphology, and microtubule growth and stability, suggests that cyclin G2 may modulate the cell cycle and cellular division processes through modulation of PP2A and centrosomal associated activities.

Keywords

Cyclin; Cell Cycle Arrest; Centrosome; Cytoskeleton; Nucleocytoplasmic; PP2A

*Correspondence to: Mary C. Horne, 2-530 BSB, 51 Newton Rd, Department of Pharmacology, University of Iowa, Iowa City, IA 52242-1109, Phone: (319) 335-8267, FAX: (319) 335-8930, E-mail: mary-horne@uiowa.edu.

INTRODUCTION

Prototypical cyclins bind to and act as positive regulatory subunits for specific cyclin dependent kinases (CDKs) and thus promote cell cycle progression. All cyclins possess a characteristic "cyclin fold" containing highly conserved alpha-helical sequence regions referred to as the cyclin box and a bundle repeat [2,3]. Despite structural similarities, some cyclins and CDKs are associated with functions not directly linked to cell cycle progression, e.g., transcription and neurite outgrowth [4–6]. Cyclin G2, (G2) is an unconventional cyclin [7,8] expressed at modest levels in proliferating cells, peaking during the late S/early G_2-phase, that is significantly upregulated as cells exit the cell cycle in response to DNA damage and receptor mediated negative signaling in B-lymphocytes [7–9]. Recent reports of differential microarray analyses consistently point to G2 upregulation in parallel with cell cycle inhibition during responses to diverse growth inhibitory signals, such as heat shock, oxidative stress, hypoxia and differentiation, further supporting the hypothesis that G2 has cell cycle inhibitory functions [10–16]. Not only does endogenous G2 expression parallel cell cycle arrest, ectopic expression of G2 inhibits CDK2 activity and induces a G_1/S phase cell cycle arrest[1]. Ectopic cyclin G2 also promotes the formation of unusual nuclear DNA structures suggestive of aberrant mitosis or cytokinesis [1]. Consistent with the notion that G2 contributes to promotion of cell cycle exit is the recent finding that its gene is transcriptionally activated by the growth inhibitory transcription factor (TF), FOXO3a[17,18]. Collectively, these observations suggest that cyclin G2 is a cell cycle modulator that inhibits cellular proliferation.

Although cyclin G2 shares high identity with its homolog cyclin G1 (53%), it likely serves distinct physiologic functions. In contrast to the cyclin G1 gene [19,20], the cyclin G2 gene is not a transcriptional target of p53 [7–9,21]. Moreover, ectopic cyclin G1 is primarily a nuclear protein, whereas tagged cyclin G2 is largely cytoplasmic [1,21,22]. Developmental expression and tissue distribution of cyclin G1 and G2 also differ [7,8,21]. In lymphocytes cyclin G1 expression is constitutive throughout the cell cycle, whereas cyclin G2 expression oscillates, peaking in late S and early G2 phase of the cell cycle [7,8]. Among differentiated tissues, cyclin G2 expression is highest in the cerebellum, while cyclin G1 is most abundant in muscle where cyclin G2 is low [7,8]. Cyclin G2 has no known active CDK partner; but as we and others have reported, endogenous and ectopically expressed cyclin G2 forms an active complex with protein phosphatase 2A (PP2A) [1,23]. Ectopically expressed cyclin G2 colocalizes with PP2A regulatory B' and catalytic C subunits in detergent resistant cytoplasmic complexes often localized to distinct perinuclear dots in the cytoplasm and occasionally in the nucleus [1].

PP2A is a highly conserved serine/threonine phosphatase essential for numerous cellular functions from signal transduction to translational control, endosome trafficking, cell cycle and cytoskeletal regulation [24]. The various regulatory B-type subunits direct PP2A to distinct subcellular localizations and modulate its substrate specificity [24–27]. A role for PP2A in regulation of cytoskeletal associated activities is suggested by the observations that a portion of total PP2A/C is localized to microtubules (MTs), intermediate filaments and centrosomes [24,26,28]. PP2A directly interacts with the centrosomal scaffolding protein, CG-NAP (AKAP450)[29]. General inhibition of serine/threonine phosphatases in mammalian CHO cells induces abnormal centrosome duplication and aberrant mitosis [30]. Work in *Drosophila* suggests that PP2A is required for centrosomal function and coupling of nuclear and centrosomal cycles [31]. Similarly, in the eukaryotic amoeba *Dictyostelium*, B-type subunits are prominently localized to centrosomes [32]. Furthermore, the single *S. cerevisiae* B' subunit (Rts1p) and the two *S. pombe* B' subunits (Par1p and Par2p) localize at spindle pole bodies, which are yeast equivalents of centrosomes, and at the medial ring of the developing septum of late anaphase cells. Importantly, deletion of par1, par2 and rts1 all lead to septation defects [33–36]. Accordingly, cyclin G2 could influence the activity or subcellular distribution of the PP2A B'/C complexes to regulate centrosomal function and cytokinesis.

The centrosome cycle of duplication, separation, and microtubule (MT) nucleation is integrally linked to the cell cycle [37–40]. Duplication occurs once during each cell cycle and is dependent on active cyclin/CDK2 complexes [38,41–43]. If centrosomes are experimentally ablated, somatic cells can still form mitotic spindles, but half of the cells fail to complete a normal cytokinesis and arrest in the G_1-phase [37,44,45]. In Drosophila, defects in DNA are relayed to the centrosome leading to centrosomal and spindle abnormalities, which are hypothesized to be part of a checkpoint for culling of damaged nuclei [46]. Furthermore, centrosomal abnormalities in cancer cells have been frequently observed [47–51].

A functional consequence of high cyclin G2 expression may be a change in the balance or local concentration of distinct PP2A complexes. This could lead to alterations in cytoskeletal networks and signal transduction involved in cell cycle regulation and cell division. Though evidence suggests that cyclin G2 modulates cell cycle arrest responses, little is known about the localization of endogenous cyclin G2 or the effect of elevated cyclin G2 on cellular physiology. Here we report for the first time that ectopic and endogenous cyclin G2 colocalizes with PP2A at centrosomal MTOCs, and copurifies with isolated centrosomes. We present novel findings showing that ectopic cyclin G2 expression induces the formation of MT bundles resistant to MT destabilizing agents, and inhibits regrowth of MTs from centrosomes. We define the cyclin G2 sequences required for G2 centrosomal localization to a 100 AA carboxyterminal region. Moreover, we provide key evidence that both endogenous and ectopic cyclin G2 are CRM1 regulated nucleocytoplasmic shuttling proteins. Finally, we determined that the cyclin G2-induced cell cycle arrest requires the presence of intact alleles for another nucleocytoplasmic shuttling and centrosome-associated protein linked to the cell cycle, p53. Together our studies point to a role for cyclin G2/PP2A complexes in the regulation of activities associated with centrosomal functions and provide a mechanism through which cyclin G2 up-regulation could contribute to cell cycle inhibition.

MATERIALS AND METHODS

Reagents and Antibodies

Protein G-Sepharose, horseradish peroxidase (HRP)-conjugated protein A and enhanced chemiluminescence (ECL) detection kits were purchased from Amersham Pharmacia Biotech. The DM1A mouse anti-α-tubulin monoclonal antibody was obtained from NeoMarkers (Fremont, CA), the sheep anti-α-tubulin was purchased from Bethyl Laboratories (Montgomery, TX), mouse anti-γ-tubulin (clone GTU-88), and Leptomycin B from Sigma (St. Louis, MO). Mouse anti-PP2A/C and anti-MAP 2B monoclonal antibodies were from Transduction Laboratories (Lexington, KY). Sheep anti-PP2A/C antiserum was obtained from ExAlpha Biologicals (Boston, MA) and the respective antibodies were affinity purified on affinity resins to which human PP2A/C-GST had been cross-linked [1]. Alexa 488, 568 and 660 conjugated secondary antibodies, the fluorescent DNA dye TOTO-3, and Alexa-660 conjugated phalloidin were purchased from Molecular Probes (Eugene, OR). HRP-conjugated donkey anti-sheep IgG, fluorescein isothiocyanate (FITC)-conjugated donkey anti-rabbit and anti-mouse IgG, lissamine rhodamine sulfonyl chloride (LRSC)-conjugated donkey anti-rabbit and anti-mouse, were from Jackson ImmunoResearch (West Grove, PA), and HRP-conjugated goat anti-mouse IgG was from BioRad (Hercules, CA). The 14G2 monoclonal anti-AKAP350 antibody was a generous gift from J. R. Goldenring (Medical College of Georgia), the polyclonal rabbit anti-APC antiserum was kindly provided by A. I. M. Barth (Stanford University School of Medicine), and the UM225 pericentrin antibody was a kind gift of S. J. Doxsey (University of Massachusetts Medical School). All other reagents were of standard quality from established suppliers.

Immunogen Preparation, Antibody Production, Affinity Purification and Testing

Complimentary DNA templates encoding the conserved core 99–511 amino acid domain of rabbit PP2A/B' subunits were amplified by PCR using oligonucleotides. The forward (5'GCG AGA TCT GAT ATC AAC GCC GAG GAG GCG CAG CCG3') and reverse primer (5'GC GTC GAC GGT ACC TCA GAG AGC CTC CTG GCT GGC3') contained engineered endonuclease restriction sites (BglII and EcoRV in forward, SalI and KpnI in reverse primer) for subcloning in frame with a 5' nucleotide sequence encoding glutathione-S-transferase (GST) as described [1]. GST fusion proteins were expressed, purified, and used to immunize New Zealand White rabbits as described. Polyclonal antibodies were affinity purified as described [1]. The affinity and specificity of the antibodies were tested by immunoprecipitation and immunoblotting of HA-tagged PP2A B' subunits expressed in HEK cells [1] and brain lysate [52]. This pan-specific antibody specifically detects the HA-tagged forms expressed in HEK cells as well as several endogenous B' subunit isotypes ranging from 52–72 kDa present in brain lysate.

Expression Constructs and Transient Transfection of Cells

HEK293, COS-7, and U2OS cells were cultured in DMEM (Gibco BRL), CHO cells in HAMS-F12 (Cellgrow), HCT116 [53] in McCoy's 5A (Gibco BRL) supplemented with 10% heat-inactivated fetal bovine serum (Cellgrow), 2 mM L-glutamine, 1 mM sodium pyruvate, at 37° C in a humidified chamber with 5% CO_2. Cultures were plated at 20–30% and maintained at 50–90% confluency. The DNA constructs for expression of V5 epitope tagged cyclin G2 and cyclin G2-GFP fusion proteins in mammalian cells have been described [1]. The cyclin G2 deletion and truncation constructs were prepared either by PCR amplification of murine cyclin G2 cDNAs using modified oligonucleotide primers or by restriction endonuclease fragment isolation and subcloning into pcDNA3 or pEGFP-N1. In the case of PCR amplification of cDNAs, restriction endonuclease sites were engineered in the forward and reverse primers, HindIII/PstI for the 1–140 AA construct and HindIII/BglII for the 140–240 AA construct. The forward primer contained an optimal Kozak translation initiation sequence; the reverse primer lacked the antisense sequence for an in frame stop codon allowing subcloning of G2 in frame with the GFP sequence. All constructs were verified by DNA sequencing. The YFP-tubulin expression construct was purchased from Clonetech (Palo Alto, CA). Dr. Sean Munro (MRC, Cambridge, England) kindly provided the expression vectors encoding the RFP-pericentrin PACT domain, the GFP fused AKAP450 C-terminal region [54], and the GFP-tagged centrin expression construct [55] was a gift of Dr. Jeffrey Salisbury (Mayo Clinic, Rochester, MN)

Paclitaxel-mediated Microtubule Reassembly and Purification

HEK293 cells were transiently transfected using a modified calcium phosphate precipitation protocol [56] and CHO cells using Lipofectamine [Invitrogen, Carlsbad, CA]) with one of the above pcDNA3-cyclin G2 expression constructs with or without expression constructs for the N-terminally HA tagged PP2A/C subunit [HA-PP2A/C in pcDNA3+ kindly provided by Dr. Brian E. Wadzinski, Vanderbilt University, Nashville, TN [57]] as described [1]. Cells were harvested 24–36 hours post-transfection. MT isolation from the transfected cell cultures was done according to the protocol established by RB Vallee [58]. MT reassembly and isolation from neonatal rat cerebellum was performed as described [59]. In both cases, the final MT pellet was washed two additional times by repeating the last sedimentation through a sucrose cushion as described [59]. The final washed MT pellet is therefore denoted P5.

Immunofluorescence Confocal Microscopy

CHO, COS-7, U2OS, and MCF-7 cells were seeded at $1.2x10^5$ cells/35 mm well onto a 22 mm-square glass coverslip coated with 10 μg/ml collagen and 1μg/ml poly-L-lysine (Sigma). Cells were grown for 14–18 hours before transfection with Lipofectamine (Gibco BRL) or

Lipofectamine 2000 per manufacturer's instruction. Coverslips were removed 26–48 hours after transfection and rinsed with PBS and immediately fixed with 4% paraformaldehyde for 15 minutes at RT or ice-cold MeOH at −20°C. For removal of soluble proteins and cellular lipids, coverslips were rinsed in the MT stabilizing buffer PHEM (45 mM PIPES, 45 mM HEPES, 10 mM EGTA, 5 mM $MgCl_2$, pH 6.9), pre-extracted for 90 seconds in PHEM buffer containing 0.1% Triton X-100, and rapidly rinsed in PHEM buffer immediately prior to fixation as described [60]. After fixation, the coverslips were rinsed in PBS and stored at 4°C in PBS plus 0.02% sodium azide. Specimens were permeabilized, stained, and mounted as described [1]. Images were collected by confocal microscopy using a Bio-Rad MRC 1024 confocal microscope with a krypton/argon mixed gas laser providing 488, 568, and 647 nm laser lines. To minimize the possibility of non-specific labeling, cross-reactivity of secondary antibodies with primary antibodies, and bleed through from one channel into another, control experiments were performed and signals from each channel were collected sequentially.

Microtubule Stability and Regrowth Assays

Cells were grown on poly-L-lysine and collagen coated coverslips in 35 mm 6-well plates and transfected using lipofectamine reagent as described above. Nocodazole (3 μM) was added to the media 24 hours post-transfection and incubated at 37°C for 30 minutes to 4 hours. Subsequently, the coverslips were washed three times in PBS at 4°C and placed in warm drug-free media for 3–15 minutes before they were fixed in 4% paraformaldehyde at RT or 100% MeOH at −20°C as described above.

Cellular Fractionation

Preparation of soluble and insoluble proteins was performed as described by Moudjou et al., and Paoletti et al., [61,62], with the following modifications. Briefly, U2OS cells were plated at a density of $1x10^5$ cells/ml followed by calcium phosphate mediated transfection on day 2. Cyclin G2V5His transfected or control nontransfected cells were harvested 72 hours post-transfection, followed by a PBS wash and lysis in PHEM buffer containing 1% Triton X-100 and protease inhibitors (1mg/ml leupeptin, 1mg/ml pepstatin, and 1mg/ml aprotinin). Cells were centrifuged at 300 g to pellet insoluble proteins. The cell pellet was washed in PHEM buffer and solubilized in 1 volume of SDS-PAGE sample buffer (SSB). To precipitate soluble proteins present in the supernatant from the centrifugation step, 9 volumes of methanol was added to the supernatant and incubated for 1 hour at 4°C. The precipitated proteins were pelleted by centrifugation at 300 g, washed in PHEM buffer, and solubilized in an equivalent volume of SSB.

Centrosome Amplification and its Release in Intact Cells

Hydroxyurea (HU) amplification of centrosomes from U2OS cells was carried out as described by Balczon et al., [63] with the following modifications. U2OS cells were plated at a density of $1x10^5$ cells/ml and lipofectamine-mediated transfection of RFP pericentrin and YFP tubulin was performed on day 2. Twenty-four hours post-transfection, cells were treated with 4 mM HU for an additional 48 h. Cells were then fixed in MeOH as above. As controls, identical procedure was carried out in the absence of HU. These cells were fixed on day 3 to prevent overgrowth. A third set of cells was subjected to release from the HU arrest with 5 mM caffeine for 5 hours. Cells on coverslips from each set were immunostained with the rabbit polyclonal antibody against cyclin G2 and images were collected by confocal immunofluorescence microscopy.

Centrosome Isolation and In Vitro Microtubule Nucleation Assay

Centrosomes were isolated from U2OS cells according to the method described by Moudjou and Bornens [61,64] with the following modifications. A 250 ml culture of detached, mono-

dispersed U2OS cells ($8x10^5$-$1x10^6$cells/ml) were incubated with 50 μl of 1 mM nocodazole and 50 μl of 5 mg/ml cytochalasin D for 1 hour at 37°C, rinsed in TBS buffer, and lysed with 1 mM HEPES, pH 7.2, 0.5% NP-40, 0.5 mM $MgCl_2$, and 0.1% β-mercaptoethanol. Cell debris and nuclei were removed by centrifugation at 2,500 g for 10 minutes. The filtered supernatant was incubated with 10 mM HEPES and 1μg/ml DNase 1 (Roche) for 30 minutes followed by centrifugation through a discontinuous sucrose density gradient (2 ml 65%, 1 ml 50% and 1 ml 40% sucrose, wt/wt) at 40,000 g for 1 hour. Fractions of 0.2 to 0.3 ml were collected from the bottom, frozen in liquid nitrogen and stored at −80°C. For immunoblotting, 0.1 ml of each fraction was diluted in 1 ml 10 mM PIPES at pH 6.9 followed by centrifugation at 16,000 g for 20 min to sediment the centrosomes, and then dissolved in SDS sample buffer.

The functional ability of the isolated centrosomes to promote MT nucleation was tested as described by Moudjou and Bornens (1998) with the following modifications. A 10 μl aliquot of each centrosome fraction was incubated with purified α and β tubulin dimers (Cytoskeleton) at 2.5 mg/ml and 1 mM GTP in RG2 buffer (80 mM PIPES, pH 6.8, 1 mM $MgCl_2$, 1 mM EGTA) for 8 minutes at 37°C. MTs and MTOCs were fixed with 1% glutaraldehyde at 25°C for 3 minutes and sedimented through a 25% glycerol solution in RG2 buffer onto glass coverslips. Coverslips were then treated with 1% Triton X-100 in RG2 buffer and fixed in MeOH at −20°C for 6–8 minutes. For immunofluorescence analysis, coverslips were co-immunostained with sheep anti α–tubulin, mouse anti γ-tubulin, and rabbit anti cyclin G2.

Cell Cycle Analysis by Fluorescence Activated Cell Sorting (FACS) and Flow Cytometry

The DNA distribution profiles of GFP-cyclin G2 and GFP expressing as well as nonexpressing cells were determined through a combination of cell sorting and flow cytometry using a dual laser cytometer (Becton Dickinson, San Jose, CA) as described [1]. The individual cells from each of these segregated populations were then analyzed for their DNA content and cell cycle profile using FlowJo 4.3 analysis software [1].

RESULTS

Ectopic Cyclin G2 Expression Alters Microtubule Stability and Regrowth

We reported that ectopic cyclin G2 expression induces a G_1/S- phase cell cycle arrest, and that >30% of ectopic G2 expressors exhibited aberrant nuclei suggestive of a defective mitotic or cytokinetic process [1]. We noted that ectopic G2 was detergent resistant, remaining in cells pre-extracted with Triton X-100 prior to fixation [1], and hypothesized that a portion of cyclin G2 associates with cytoskeletal elements. To investigate a possible link between G2 modulation of the cell cycle and a cytoskeletal association, we examined the effects of cyclin G2 expression on MT networks. We found that cells ectopically expressing G2, exhibited not only unusual DNA structures, but also contained aberrant MT networks not seen in GFP alone control cells. These MT structures were inconsistent with either a normal interphase array or functional mitotic spindles (see Figs. 1 and 9). The aberrant MT structures were suggestive of the stabilized MT polymer bundles observed upon ectopic expression of MT associated proteins (MAPs) [65,66]. To test the hypothesis that high cyclin G2 expression influences MT stability, we examined the effect of ectopic G2 expression on the sensitivity of MTs to the MT disrupting agent, nocodazole. Transfected cultures grown on coverslips were treated with nocodazole for 15 minutes, washed with PBS, and released into drug-free media for 3 minutes prior to fixation. Cells were stained with antibodies against α-tubulin and DNA dyes, to reveal MT arrays and nuclear DNA (Fig. 1A). As expected, untransfected and transfected control cells did not exhibit normal interphase arrays of long MT polymers but contained starbursts of new MTs grown from perinuclear MTOCs. In contrast, the vast majority of cyclin G2-GFP expressing cells exhibited nocodazole resistant perinuclear MT bundles (Fig. 1A). Additionally, in cells undergoing cytokinesis, we observed nocodazole-resistant MT bundles

surrounding the nascent nuclei along with intact MTs in the cytokinetic bridge. A cyclin G2GFP dot-like structure, reminiscent of a migrating centriole, was prominent at the bridge. Cultures transfected for expression of V5 epitope-tagged cyclin G2 were treated with nocodazole for 30 minutes, pre-extracted with Triton X-100 for 90 seconds to remove soluble material and immediately fixed. Non-transfected cells were virtually devoid of MT polymers, but cyclin G2 expressing cells contained circular bundles of stabilized MTs surrounding the nucleus that overlapped with cyclin G2 staining (Fig. 1B).

As MT depolymerization appeared to be inhibited in cells abundantly expressing G2, we extended the duration of nocodazole treatments. After 1 h, the majority of cyclin G2 expressing cells lacked MT polymer bundles and by 2 h of treatment, virtually all of the MT polymers were absent in cyclin G2 expressors (see below and data not shown). We tested the ability of cyclin G2 expressors devoid of polymers to repolymerize MTs upon drug washout. Following a 1h nocodazole block, cells were rinsed and released from drug for 3 min, pre-extracted as before, fixed and stained for α-tubulin and DNA. In contrast to non-transfected and GFP expressing control cells, the preponderance of cells expressing abundant levels of cyclin G2 with either a GFP or V5 epitope-tag did not exhibit the typical burst of MT regrowth from MTOCs (Fig. 1 C, D). In addition, unusual DNA structures not typical of either interphase or normal mitotic cells were present in most of the high cyclin G2 expressors, but were rarely seen in control cells. Together, these results suggest that the ectopic cyclin G2-mediated cell cycle arrest we observed may be downstream of an aberrant mitotic or cytokinetic process that occurs as a consequence of G2-induced dysregulation of MT stability.

Endogenous and Ectopic Cyclin G2 distributes to Detergent-Resistant Subcellular Fractions

Epitope-tagged cyclin G2 and co-expressed PP2A subunits are largely resistant to Triton X-100 pre-extraction and colocalize to a high degree [1]. These earlier observations also suggested that G2 and its binding partner PP2A are associated with MTOCs and MTs, but the relative amounts of cyclin G2 in the detergent-insoluble cytoskeletal versus soluble cytoplasmic fraction remained to be determined. More than 50% of γ-tubulin and centrin, two critical components of the centrosome, are distributed to the Triton X-100 soluble cytoplasmic fraction in cycling cells, though this distribution is influenced by the cell-cycle and differentiation state of the cells [62,67,68]. Following the methods described by Moudjou et al., [67,68] and Paoletti et al., [62], we examined the relative abundance of G2 present in the soluble versus insoluble fractions of asynchronous cycling U2OS cells. Distribution of ectopic and endogenous cyclin G2 in each fraction was analyzed by IB and compared to γ-tubulin (Fig. 2). Consistent with our immunocytochemistry analysis of transiently transfected cell populations, we determined that a significant portion of ectopic cyclin G2 distributes to the Triton X-100 insoluble fraction (Fig. 2A). Importantly, our studies also showed that the majority of endogenous G2 in cycling U2OS cells partitions to the detergent insoluble fraction. Moreover, in comparison to γ-tubulin, proportionally more of endogenous G2 was present in the Triton X-100 insoluble fraction (Fig. 2B).

Cyclin G2 Copurifies with Paclitaxel-Stabilized Microtubules

Ectopic and endogenous cyclin G2 partitions to detergent resistant compartments, and ectopic G2 often colocalizes with bundles of nocodazole resistant MTs, or distributes as puncta or filamentous structures partially colocalizing with MT arrays (Fig. 3A). Thus we tested whether cyclin G2 associates with Paclitaxel-stabilized MTs reassembled and isolated from cytosolic rat brain extracts or from transfected cell lysates (Fig 3). Like the neuronal MAP2B, endogenous cyclin G2 copurified with reassembled and Paclitaxel-stabilized MTs from cytosolic rat brain extracts (Fig. 3B). Moreover, similar to the MT-associated protein, MAP4, cyclin G2 copurified with Paclitaxel-stabilized MTs that were reassembled from homogenates of HEK and CHO cells ectopically expressing cyclin G2-GFP (Fig. 3C, D). In contrast, GFP

did not copurify with MTs reassembled from transfected control cells (3C, data not shown), suggesting that the association of cyclin G2 with MTs is specific (Fig. 3C, D). Because cyclin G2 interacts with PP2A/C [1] and PP2A/C associates with MTs [26,28,69] we reprobed the blots with antibodies against PP2A/C. As expected, endogenous PP2A/C copurified with MTs (Fig. 3B, D). To determine whether the abundance of PP2A/C influences the co-purification of G2 with MTs, or vice versa, we isolated Paclitaxel-stabilized MTs from cultures expressing cyclin G2-GFP co-transfected with or without HA-PP2A/C. Modest overexpression of ectopic PP2A/C promoted the association of cyclin G2 with assembled MTs (Fig. 3D; compare left and right panels). These results indicate that a portion of cyclin G2 associates either directly or indirectly with the MT cytoskeleton and that cyclin G2 could influence MT stability via its association with PP2A.

Ectopic Cyclin G2 and PP2A/C Localizes to Centrosomes

In a significant population (~ 20–30%) of cells, transiently transfected cyclin G2 concentrated at bright perinuclear dots, suggestive of a centrosomal localization (Fig. 4). To determine whether these dot-like structures were indeed at centrosomes/MTOCs, we treated cells for 0.5 to 4 h with nocodazole followed by release into drug-free media for 2 to 10 min, and then fixed and immunostained. Confocal microscopy of cells stained with antibodies against α-tubulin and pericentrin indicated that the concentrated perinuclear dots of cyclin G2-GFP were colocalized at the center of MT bursts emanating from pericentrin positive dots (Fig. 4A). Staining of cells with anti-γ-tubulin antibodies indicated similar results (Fig. 4C). Thus a significant portion of ectopic cyclin G2 localizes to centrosomal MTOCs.

As we had previously observed cyclin G2 colocalizing with a portion of HA-PP2A/C at perinuclear foci, we performed nocodazole block and release experiments similar to those described above. Cyclin G2-GFP and HA-PP2A/C co-transfected CHO cells were treated with nocodazole followed by pre-extraction with 0.5% Triton-X 100 in PHEM buffer prior to fixation. Immunolabeling of the MTs and PP2A/C indicated that cells expressing low to moderate amounts of cyclin G2-GFP had a significant proportion of PP2A/C colocalized with cyclin G2 at MT foci suggestive of MTOC/centrosomes (Fig. 4D). Collectively, these results indicate that cyclin G2-PP2A complexes are preferentially localized to centrosomes at some period during interphase cell cycle transitions.

Endogenous Cyclin G2 Colocalizes with Centrosomes

Additional boosting of our rabbits producing anti-cyclin G2 antisera [1] yielded higher titer affinity purified antibodies, which when used for immunoblotting of U2OS cell lysates detected a single band at ~42 kDa, the predicted molecular mass of endogenous cyclin G2 (Fig. 5A). Co-staining of untransfected U2OS cells with this antibody and anti-α-tubulin revealed a prominent anti-cyclin G2 immunosignal that coincided with spindle poles, indicating that endogenous cyclin G2 localizes to the centrosomal region in these cells (Fig. 5B). To confirm that these foci correspond to centrosomes, we transfected U2OS cells with expression plasmids for RFP-pericentrin and YFP-α-tubulin, and applied (4mM) hydroxyurea (HU) to induce S-phase arrest and centrosome amplification (5C, top) followed by a (5mM) caffeine release (5C, bottom) to allow the coalesced centrosomes to separate [63,70,71] and examined them by confocal immunofluorescence microscopy. The cyclin G2 antibody labeled multiple RFP-pericentrin foci of amplified centrosomes (Fig. 5C). Further co-immunostaining of U2OS cells treated with nocodazole for 4h followed by a 5 min release, and fixation in MeOH showed anti-G2 positive foci co-labeled with antibodies directed against the centrosomal AKAP, AKAP350 (AKAP450 or CG-NAP) (Fig. 5D). Thus, endogenous cyclin G2 colocalizes to a large degree with the centrosome in mitotic and interphase cells of unperturbed U2OS cell cultures. These results were extended by co-localization of cyclin G2 positive foci with different centrosomal markers in a variety of cell types, including MCF-7 cells stained with

antibodies against the centrosomal marker, γ-tubulin (Fig. 5E). Similar results were observed in HCT116 and MCF10a cells (data not shown).

Endogenous Cyclin G2 and PP2A Co-purify with Isolated Centrosomes

To determine whether cyclin G2 is tightly associated with the centrosome in U2OS cells, we performed subcellular fractionation as described [61], obtained purified isolates enriched with centrosomes, and tested for cyclin G2 co-enrichment. Immunoblotting with anti-γ–tubulin (Fig. 6A) indicated a peak signal in the sucrose gradient fractions at ~60%, the concentration previously reported for peak centrosome enrichment [61]. Cyclin G2 immunosignals on the blot were maximal in the lanes containing the peak γ-tubulin signal (Fig 6A). Also, note the comparable distribution through the sucrose gradient of both the cyclin G2 and the peak γ-tubulin immunosignals with another known centrosome localized protein, adenomatous polyposis coli (APC) [72].

To confirm that cyclin G2 was associated with isolated centrosomes present in the corresponding sucrose gradient fractions, we sedimented selected peak and non-peak control fractions onto coverslips, fixed, and immunostained with antibodies against γ-tubulin and cyclin G2. Depicted in the merge as yellow is cyclin G2 foci colabeled at γ-tubulin positive centrosomes from peak fractions (Fig. 6B). We also incubated selected fractions shown in Fig. 6C from a repeat isolation experiment with tubulin and GTP to nucleate MTs, sedimented the asters and centrosomes onto coverslips, fixed, and immunolabeled them with antibodies to α- and γ-tubulin and cyclin G2. Following staining of these isolates with fluorescently tagged secondary antibodies; sequential optical section images were captured by confocal microscopy. Anti-cyclin G2 antibodies labeled γ-tubulin positive centrosomes, some of which showed clear aster formation (Fig. 6D, arrows; inserts show close-up of these asters). As the γ-tubulin ring complex (γ-TuRC) in PCM of centrosomes also contains α-tubulin, the anti-α-tubulin antibody labeled centrosomes with and without MT asters (Fig. 6D). These observations show that endogenous cyclin G*2* closely associates with the centrosome, where it may regulate one or more of its functions.

Proteomic analysis has indicated that PP2A/C is a centrosomal protein [32,73]. Our immunoblot analysis of sucrose fractions is consistent with these reports and as PP2A/B' and PP2A/C subunits copurified with the cyclin G2 and γ-tubulin enriched centrosomal fractions (Fig. 6C and data not shown). As we have previously seen a colocalization of PP2A subunits with ectopic cyclin G2 at centrosomes (Fig. 4D and data not shown), our results collectively suggest that cyclin G2 may be in a complex together with PP2A at centrosomes.

Expression of AKAP450 c-terminal PACT domain dissociates endogenous cyclin G2 from the centrosome

A number of kinases, phosphatases, including PP2A and other regulatory proteins are localized at centrosomes [37,39,40], through association with large centrosomal scaffolding A kinase-anchor proteins, (AKAPs). Our previous results and data presented above suggest that cyclin G2 may associate in a complex with centrosomal PP2A. As it has been demonstrated that PP2A/C is a centrosomal protein [32,73] that associates with the centrosomal scaffolding protein CG-NAP/AKAP450 [29], we hypothesize that cyclin G2-PP2A complexes could be anchored at centrosomes via association with AKAP450. To test this hypothesis we took advantage of the observations that ectopic expression of the AKAP450 c-terminal centrosomal targeting PACT domain [40,54] displaces endogenous AKAP450 and its associated signaling enzymes from the centrosome [40,54,74]. We transfected U2OS and MCF-7 cells with this AKAP450 c-term PACT domain tagged with GFP [54], and examined the centrosomal localization of endogenous cyclin G2 at microtubule organizing centers and γ-tubulin labeled centrosomes via immunofluorescence confocal microscopy (Fig. 7). Results indicate that centrosomal

localization of ctAKAP450-GFP leads to a loss of endogenous cyclin G2 from these MTOCs/centrosomes (Fig. 7A, B). This suggest that a majority of centrosomal cyclin G2 associates with CG-NAP/AKAP450 and is consistent with the idea that cyclin G2-PP2A complexes are anchored together at centrosomes via association with AKAP450.

Endogenous Cyclin G2 enrichment is at a single, MT-array-associated centriole, suggesting that G2 primarily localizes to the Mature "Mother" Centriole (MC)

Centrin, a 20kDa protein required for centrosome duplication, is rapidly localized to the distal lumen of developing centrioles and stably maintained in the lumen of the developed daughter centriole (DC) and MC [39,62,75]. Because centrin is integral to each centriole of a centrosomal pair, it is often used as a cytological marker for centrosomal maturity and for determining the cell cycle stage based on the number and position of the centrioles. Notably, other studies suggest that a majority of centrosomal AKAP450 distributes to the MC [45,74,76].

Here we utilized GFP-labeled centrin to further investigate where cyclin G2 is localized with respect to centriole pairs and thereby gain more insight into the centrosomal activity or function that might be influenced by cyclin G2. Cyclin G2 closely and preferentially associated with the large centrioles that are at the foci of MT arrays, typically the MCs (Fig. 8) [39,76]. Cyclin G2 staining did not overlap with the smaller, MT-free centrioles that correspond to the DCs. These findings are in agreement with our observation of prominent cyclin G2-GFP dots on midbody MT bridges between cell pairs in the final stages of cytokinesis (see Figs. 1A and 3A), as the MC migrates to this position just prior to abscission. The MC possesses appendages that act as primary anchors for stable radial MT arrays and is the preferential site for PCM accumulation and localization of signaling molecules. Thus the MC is usually larger than the simpler DC until late G_2. Therefore, the appearance of cyclin G2 staining as a larger dot overlaying the centrin-GFP signal at the center of a radial MT array (Fig. 8D) is consistent with cyclin G2 association with either the anchoring sites or the PCM surrounding the MC.

Carboxyterminus of Cyclin G2 is required for Localization to Centrosomes

We have previously shown that the carboxy-terminal region 142–344 is required for association with PP2A and induction of ectopic cyclin G2-mediated cell cycle arrest [1]. To determine the region of cyclin G2 that directs it to the centrosome, we compared the localization of GFP fused to full length, N-terminal, C-terminal, and internal cyclin G2 polypeptides relative to the centrosomal marker γ-tubulin and to re-growing MTs after nocodazole block and release (Fig. 9). The first 140 amino acids of cyclin G2 fused to GFP exhibited a rather diffuse staining pattern (Fig. 9B) and was largely extracted by 0.5% Triton X-100 (data not shown), similar to GFP alone and in contrast to full length and the more C-terminal cyclin G2 constructs. Fixation with methanol partially extracts soluble proteins, but left a detectable level of 1–140 cyclin G2-GFP behind. This property allowed us to identify transfected cells, obtain clean γ-tubulin staining of the centrosome, and by α-tubulin labeling, we also detected MT burst of regrowth from the MTOC following a nocodazole block and release. We determined that the N-terminal region of G2 could not efficiently direct GFP to centrosomes (Fig. 9A, B). In contrast, the C-terminal half of cyclin G2 (142–344) did target GFP to the centrosome. Cells expressing 142–344 cyclin G2-GFP displayed bright, conspicuous concentrations of the fusion protein at γ-tubulin positive dots and were often multinucleated (Fig. 9C). The larger the accumulation of cyclin G2-GFP fusion protein, the lower the signal intensity for the γ- and α-tubulin staining, suggesting that MT regrowth from the MTOC is inhibited or delayed by this construct. Alternatively, in some cases the centrosomal region may contain a very high concentration of the fusion protein that hinders antibody penetration. Finally, we tested the possibility that a shorter centrosomal targeting sequence laid within the first half of the C-terminal polypeptide. The 140–240 cyclin G2-GFP fusion proteins were frequently found concentrated at centrosomes (Fig. 9D), suggesting that this 100 amino acid internal region of cyclin G2 just

C-terminal to the cyclin box possesses a cyclin G2-specific polypeptide sequence sufficient to target GFP to centrosomes.

Nucleocytoplasmic shuttling of cyclin G2

In contrast to cyclin G1-GFP, G2-GFP is mainly cytoplasmic, localized at centrosomes and cytoskeletal sites (see Fig 10A). However, when ectopically co-expressed with interacting proteins containing nuclear localization signal (NLS) sequences such as PP2A B' subunits or Mdm2 [1,22], and in small proportion of singly transfected asynchronous cells, a significant portion of G2-GFP can be detected in the nucleus (data not shown, and Fig. 10B). As both G2-GFP (69 kDa) and G1-GFP (61 kDa) are > 60 kDa, simple diffusion across nuclear membranes is likely insufficient for either's nuclear localization. To investigate the regulation of cyclin G2 subcellular trafficking we tested whether cyclin G2 accumulation within the nucleus is influenced by the activity of the nuclear export protein CRM1/exportin. NIH3T3 cells transfected with G2-GFP or GFP control expression vectors were treated with vehicle alone or CRM1/exportin inhibitor, Leptomycin B (LMB), for 9 h and the relative abundance of the GFP signal in the cytoplasm versus the nucleus was observed. In contrast to GFP controls, the number of NIH3T3 cells with intense nuclear G2-GFP was significantly increased within 9 h, suggesting that G2 is exported from the nucleus in a CRM1 dependent manner (Fig. 10B and data not shown). In contrast, the localization of G1-GFP was unaltered although a moderate increase in nuclear intensity was detectable (data not shown). Treatment of untransfected U2OS and NIH3T3 cells with 6ng/ml LMB for 6 hours and staining for endogenous G2 and MTs showed a build-up of G2 immunoreactivity in the nuclei of LMB- but not mock-treated cells (see Fig. 10C and data not shown). In light of our observations that G2 can interact with PP2A B' and C subunits [1], p53 and Mdm2 [22], and G2 colocalizes with Mdm2 and PP2A/C in the nucleus when ectopically expressed ([1] and data not shown), these results suggest that G2, possibly when elevated in response to growth inhibitory signals, may shuttle between the nucleus and the cytoplasm/cytoskeleton, depending on the signaling pathways engaged and its association with specific binding partners.

Cyclin G2 Induced Cell Cycle Arrest is p53-dependent, and partially dependent on p21

Cyclin G2 is normally at low levels in cycling cells but increased in response to DNA damage and growth inhibitory signaling [7–9]. We tested the effect of ectopic cyclin G2 expression in U2OS and HCT116 cells, cell lines with defined p53 alleles and function [53], to determine whether increased cyclin G2 in these cells is growth inhibitory and whether this requires p53 function. We expressed GFP tagged full length and C-terminal cyclin G2 polypeptides or control GFP in these cells, stained the DNA of live cells with the cell permeable DNA dye Hoechst 33342, and analyzed the DNA content profile in GFP expressors and non-expressors isolated from the same cultures as described [1]. The cell cycle of U2OS cells expressing either full length or a cyclin G2 C-terminal fragment was inhibited in comparison to non-expressors and GFP expressing control cells, consistent with previous results (Fig. 11A, top row). Likewise, HCT116 cells homozygous for wild type p53 expressing full length and C-terminal cyclin G2 exhibited a G_1-phase cell cycle arrest while the control cells had DNA content profiles typical of an asynchronous cycling cell population (Fig. 11A, middle row). Notably, p53 homozygous null HCT116 cells expressing either full length cyclin G2 or the cyclin G2 C-terminus were not cell cycle inhibited and displayed DNA histograms very similar to the control populations of cycling cells (Fig. 11A, bottom row). Thus, increased cyclin G2 expression induces a p53-dependent G_1-phase cell cycle arrest. Moreover, these results indicate that the region of cyclin G2 found to interact with PP2A (residues 142–344) possesses p53-dependent cell cycle inhibitory activity that can localize to the centrosome. To begin to assess which p53-dependent downstream effectors might be required for the G2-induced cell cycle arrest, similar experiments were performed in HCT116 cells harboring intact p53 alleles, but lacking an important p53 transcriptional target and cell cycle regulatory allele, the gene

encoding the CDK inhibitor, p21. Cell cycle analysis of transiently transfected HCT116 $p21^{-/-}$ cells expressing G2-GFP indicated that in comparison to p53 null and wild type HCT116 cells, loss of p21 had only a modest intermediary effect on cyclin G2 inhibitory activity (Fig. 11B). Thus, cyclin G2-PP2A association, intact p53, and p53 downstream effectors other than p21 are required for the cyclin G2 elicited cell cycle inhibition.

DISCUSSION

In earlier reports we hypothesized that the development of aberrant nuclei in cells ectopically expressing cyclin G2 resulted from dysregulation of a late mitotic or cytokinetic process [1]. Here we show that a portion of endogenous cyclin G2, along with a binding partner, PP2A/C, copurifies with MTs and centrosomes. In addition, we show that ectopic G2 also colocalizes with centrosomes, and is distributed to a larger detergent resistant cytoskeletal compartment, and copurifies with MTs. Interestingly, upregulation of cyclin G2 expression via transient transfection results in nocodazole-resistant stabilized MTs, and dysregulation of MT polymer growth from centrosomes. We determined that endogenous cyclin G2 localization to centrosomes is disrupted when the centrosomal targeting PACT-domain of the scaffolding protein, AKAP450, is ectopically expressed. AKAP450 anchors numerous enzymes, including PP2A phosphatase on centrosomes. We show that the c-terminal region necessary for interaction with PP2A and cell cycle inhibition, is required for cyclin G2 targeting to centrosomes, and is sufficient to induce a p53-dependent cell cycle arrest. Thus the effects of ectopic cyclin G2 expression on the nuclear structure, the cell cycle, and the cytoskeleton suggest a role for the cyclin G2-PP2A/C complex in regulation of MT-associated processes central to cellular division.

A key site for coupling of the MT cytoskeleton to cell division and the cell cycle is the centrosome. It is becoming increasingly evident that the centrosome possesses not only the architecture for MT nucleation and anchoring sites for stable MT arrays, it also provides a scaffold for numerous signaling molecules that regulate processes important to mitosis, cytokinesis, and the coupling of the cell cycle to the centrosome cycle [40]. Therefore, our discovery that ectopic and endogenous cyclin G2 localizes at centrosomes and copurifies along with PP2A in centrosome-enriched subcellular fractions, implicates cyclin G2 involvement in aspects of centrosome-associated functions. As moderate to high levels of ectopic cyclin G2 protein can be antagonistic to cell cycle progression, and amino acids 140–240 of cyclin G2 are required for association with PP2A and cell cycle inhibition [1], we tested which sequence domain of G2 is sufficient for targeting GFP to the centrosome. The finding that the same 100 amino acid region of cyclin G2 is sufficient to target GFP to the centrosome suggests that cyclin G2 may also direct PP2A to the centrosome.

MT nucleation at the centrosome is promoted by a structure residing in the PCM called the γ-tubulin ring complex (γ-TuRC) [77]. In addition to structural components, regulatory proteins such as kinases, phosphatases are localized at centrosomes [37,39,40], many of which are anchored by one or both of two distinct A kinase-anchor proteins (AKAPs), AKAP450 (also known as AKAP350 or CG-NAP) and pericentrin. These AKAPs possess a conserved centrosomal targeting sequence called the PACT domain [40,54]. AKAP450 acts as a centrosomal scaffold for a variety protein kinases and phosphatases, including a subpopulation of PP2A [29,40,78–80]. Although the exact subunit composition of centrosomal PP2A, or its associated proteins and targets are not known, cyclin G2 could associate with PP2A via AKAP450. Consistent with this notion is our observation that endogenous cyclin G2 localization to the centrosome is disrupted by expression of the c-terminal PACT domain of AKAP450 (Fig. 7).

Mitotic and cytokinetic defects have been linked to dysregulated or mutated PP2A subunits in yeast, Drosophila and mammalian cells [81–84]. For example, inhibition of serine/threonine phosphatases in CHO cells induces abnormal centrosome duplication resulting in aberrant mitosis [30]. In Drosophila, loss of PP2A/C results in disorganized MT arrays, elongated MTs that fail to attach to kinetochores, and an uncoupling of the nuclear and centrosomal cycles [31]. Importantly, Rts1p, the *S. cerevisiae* B' subunit homolog, is localized to spindle pole bodies following migration to the bud neck, kinetochores and the bud neck of post-telophase cells [36]. Deletion mutants of *RTS1* in *S. cerevisiae*, or its homologs in *S. pombe*, exhibit spindle orientation and septation defects [35]. Moreover, overexpression of mammalian B' subunits in *S. cerevisiae* results in abnormal elongated cellular morphology [27]. Finally, PP2A B' subunits are localized to and bundle planar MT webs in Drosophila, and are required for planar cell polarity, in both and fly and zebrafish [69]. Thus elevated cyclin G2/PP2A complexes may modulate similar centrosomally regulated processes in mammalian cells.

PP2A activity promotes accumulation of stable MTs [85], likely via its regulation of various MAPs [28,86]. We find that ectopically expressed cyclin G2 expression induced nocodazole resistant MT bundles (Fig. 1). It is intriguing that upon nocodazole washout and regrowth of nascent MTs the most obvious colocalization of ectopic cyclin G2 with MTs occurs at their plus ends (Fig. 3A). MT stability is highly regulated by various MAPs during the highly polar processes of mitosis and cytokinesis [66,87]. Although our evidence suggests that cyclin G2 expression influences MT stability and regrowth, we do not yet know whether cyclin G2 binds together with PP2A/B' on a scaffolding protein or MAP on MTs. We do however have evidence suggesting that centrosomal localized cyclin G2, perhaps in conjunction with PP2A, associates with the centrosomal scaffolding protein, AKAP450 (Fig. 7). Through association with a distinct pool of PP2A isozymes, elevated expression of cyclin G2 could alter PP2A activity associated with centrosomes, or MAP activity associated with spindles, cytokinetic bridges of dividing cells, or overall microtubule networks. The elevated levels of cyclin G2 could influence PP2A by either sequestering or directly modulating its activity towards distinct targets. As cyclin G2 elevation in unperturbed cycling cells is normally moderate and occurs transiently during the late S/early G2 phase of the cell cycle [7,8,17], but is significantly (5–10 fold) and persistently elevated during cellular stress responses and growth inhibitory signaling ([7–9,15] and our unpublished observations), it is possible that cyclin G2 complexes could contribute to modification of centrosomal/cytoskeletal associated activities that promote cell cycle inhibition. In the case of unregulated ectopic expression of cyclin G2, in the absence of additional signals, G2 could perturb the normal activity of PP2A, or another unknown partner, which in turn could lead to dysregulation of microtubule stability and dynamics that ultimately leads to an aberrant mitosis/cytokinesis.

Most MAPs do not associate with MTs throughout their length, or during the entire cell cycle. The number of known MAPs has increased and now includes numerous plus-end binding/tracking proteins and motor proteins with microtubule stabilizing and destabilizing activity [66,88]. Information on how some of these proteins regulate microtubule stability and dynamics is beginning to emerge, though very little is known about the regulation of these new classes of MAPs themselves, including the signaling proteins and enzymes that are involved. It is conceivable that direct dephosphorylation via PP2A could play an important role. Some of the plus end-binding MAPs, such as EB1 and APC, have also been clearly localized to centrosomes [72,89,90], and ectopic expression of either induces microtubule bundling and nocodazole resistant microtubles. Interestingly, APC associates with PP2A B' subunits [91], though the importance of this association for its cytoskeletal functions is unknown. Another protein linked to cellular stress responses and regulation of cell division, survivin, localizes to multiple sites on the mitotic apparatus, including centrosomes, microtubules of the metaphase and central spindle, kinetochores, and midbodies [92,93]. Survivin has recently been found to modulate microtubule dynamics and nucleation throughout the cell cycle [92]. Notably, like

cyclin G2, ectopic expression of survivin induces microtubule bundling and inhibits regrowth of MTs from centrosomes following nocodazole washout, though the mechanism by which this occurs is not known [92].

As the major MTOC of animal cells, the centrosome comprised of a pair of centrioles surrounded by the pericentriolar material, influences many MT related functions. Use of GFP-tagged centrin along with EM studies has demonstrated that the two centrioles within an interphase centrosome appear and behave quite differently with respect to size and colocalization with MTOC [39,55,76], and this difference of centrioles marked by GFP-centrin is commonly used to help define the localization of centrosomal associated proteins[39,55, 76]. The two centrioles of a centrosome are thought to carry distinct activities, with the larger mature “mother” centriole (MC) capturing and anchoring nucleated MTs and providing important signals to the midbody that promote cytokinesis [39,76,94–96]. These functions are facilitated by the rotation and movement of the MC to the midbody prior to cytokinesis [76, 94,96,97]. Inhibition of this process is associated with cytokinetic defects [96]. We determined that endogenous cyclin G2 in U2OS cells associates primarily with the larger of two GFP-centrin-tagged centrioles that is also more closely associated with the MT array of the MTOC (Fig. 8), and speculate that cyclin G2 is primarily associated with the MC. The likelihood that cyclin G2 may function in cytokinesis is strengthened by the prominent accumulation of ectopic cyclin G2-GFP at interphase centrosomes as well as at midbody MT bridges (Figs. 1, 3A, and 4). Thus it is quite conceivable that ectopic cyclin G2, perhaps in association with PP2A, could dysregulate cytokinesis to ultimately result in incomplete or failed division and aberrant nuclei formation.

Defects in cytokinesis may lead to cells with a greater than 2N complement of chromosomes, binucleated cells, cells with supernumerary centrosomes, and ultimately genomic instability. Loss or increase in centrosome numbers often result in aberrant cytokinesis and induction of G_1-phase cell cycle arrest [44,98,99]. The growth arrest response in cells lacking centrosomes could be due to a loss of key components, whereas multiple centrosomes could provide an imbalance of these components or simply lead to improper spindle alignment, unequal partition of chromosomal DNA and a DNA damage response [37,40,50]. Alteration of centrosomal components that results in inhibition of cytokinesis and centrosome duplication has been shown to induce cell cycle arrest [74,75,100]. Both loss and overexpression of centriolin, a newly identified centrosomal component, induces cytokinetic defects and a G_1-phase cell cycle arrest [100]. Moreover, disruption of AKAP450 localization to centrosomes results in centrosomal and cytokinetic defects leading to a p53 dependent G_1-phase cell cycle arrest [74]. Relevant to our hypothesis that cyclin G2 associates with PP2A at the centrosome, a similar disruption of endogenous AKAP450 anchoring at the centrosome through ectopic expression of the AKAP450 PACT domain, results in loss of cyclin G2 immunostaining at centrosomes in U2OS and MCF-7 cells (Fig. 7).

Due to the robust arrest responses induced by cytokinetic defects, it has been postulated that this response requires p53 [74,98,101,102]. In support of our hypothesis, we determined that the G_1-phase cell cycle arrest induced by ectopic cyclin G2 expression is linked to its centrosomal targeting region and is p53-dependent. Other investigations with the same HCT116 cell lines indicate that a centrosome-intrinsic mechanism for centrosome duplication is significantly enhanced by the presence of wild-type p53 [70]. Functional centrosomes are needed not only for the fidelity of cytokinesis but also for cell cycle progression through G_1 into S-phase [44,45,103]. Accordingly, a centrosomal sensing mechanism exists that requires intrinsic factors to determine their ability to duplicate and progress into S-phase and can block reduplication of centrosomes that are not at the correct developmental stage [70,104]. Cyclin G2 localized at the centrosome may be involved in MC-associated signaling pathways (perhaps

involving the protein kinases and phosphatases associated with AKAP450) that link centrosome integrity and duplication to cell cycle progression [74].

Cyclin G2 associates with nuclear proteins containing known NLS's (e.g., PP2A/B' and p53 [1,22]) and export of endogenous and exogenous G2 from the nucleus is blocked by Leptomycin B (LMB) (see Fig. 10). Hence, its trafficking is likely not a futile cycle but rather a highly regulated and physiologically significant process. Recent studies on Ran association with AKAP450 at the centrosome show that two key centrosomal proteins, centrin and pericentrin/kendrin accumulate in the nucleus of LMB treated cells while others such as AKAP450 and ninein do not [105]. The authors propose that centrosomal localization of Ran and the nucleocytoplasmic shuttling of select centrosomal proteins could couple centrosome activity and nucleocytoplasmic exchange [105]. Keryer et al., suggest that centrosome-associated RanGTP could locally destabilize importin/centrosomal protein complexes and thus activate processes important for centrosome activities such as MT assembly, anchorage, and dynamics. Not only Ran, but also RanBP1 and Crm1, are stably present at centrosomes [106–108]. We hypothesize that regulation of CRM1-dependent export of G2 controls its functions and may impact an associated centrosomal process. Alternatively, as G2 is upregulated in responses that stabilize and activate p53 and can associates with Mdm2/PP2A complexes, it could be an important nuclear modulator of the p53-Mdm2 pathway [23,25]. Therefore, further investigation of cyclin G2 subcellular trafficking is highly warranted.

Cyclin G2 is highly expressed in human and rodent brain [7,8] where it forms catalytically active complexes with PP2A/C subunits [1]. Although we do not know which B-type subunit is present in cerebellar cyclin G2 – PP2A complexes, preliminary evidence suggests that it is a B' subunit ([57], and A.S. Arachchige-Don and M.C. Horne, unpublished observations). Differentiation signals upregulate the expression of brain specific B' subunit isoforms in neuroblastoma cells [25], which are thought to direct PP2A to particular compartments during brain development. Our findings that endogenous cyclin G2 and PP2A/C copurify with MTs (Fig. 3), and that they form enzymatically active complexes [1], suggest that cyclin G2 is involved in modulating either the subcellular localization or specificity of the PP2A/C complex, likely in conjunction with specific B' subunits. The formation of this cyclin G2 complex is inhibitory for cell cycle progression, and may be important to promote sustained exit from the cell cycle in response to corresponding inhibitory signals or cellular differentiation programs.

Our data strongly indicate that cyclin G2 is a novel centrosomal and nucleocytoplasmic shuttling protein that can modulate MT stability and affect p53-dependent cell cycle inhibition. Our studies also suggest that physiologically elevated cyclin G2 may influence mitosis or cytokinesis. In transfected cells with moderate levels of ectopic cyclin G2-GFP, the GFP signal is found as puncta decorating nascent MTs (Figs. 3A, 4A). In addition, endogenous cyclin G2 copurifies with assembled MTs (Fig. 3) and isolated centrosomes (Fig. 6). Overexpression of cyclin G2 could induce subtle changes in the subcellular distribution of PP2A B'/C complexes leading to an altered regulation of cellular division resulting in aberrant nuclei and ultimately a G_1/S-phase arrest. In light of many recent microarray analyses that point to cyclin G2 as a negative regulator of cell cycle progression [10–16], our results provide important new insight into the cellular compartments and processes wherein elevated cyclin G2 could contribute to cell cycle inhibition. The roles that cyclin G2 plays in cell cycle regulation and cell division may depend on the stage of the cell cycle, the activation of signaling pathways and association with unknown partners. It will be interesting to determine whether elevation of endogenous cyclin G2 in response to DNA damage or other signaling paradigms that upregulate G2, lead to its increased abundance at centrosomes, redistribution to MTs or accumulation in the nucleus.

Acknowledgements

We express our gratitude to Dr. Jeffrey L. Salisbury of the Mayo Clinic, Rochester, MN for advice, discussion, and the kind gift of the GFP-centrin expression vector, Dr. Sean Munro (MRC, Cambridge, England) for the generous gift of the RFP-pericentrin and GFP-AKAP450 PACT domain expression constructs, Dr. James Goldenring (Medical College of Georgia) for the helpful donation of the monoclonal anti-AKAP450 antibody 14G2, Dr. Stephen Doxsey (University of Massachusetts Medical School) for the UM225 pericentrin antibody, Dr. Angela Barth (Stanford University School of Medicine) for the polyclonal rabbit anti-APC antiserum, and Dr. Bert Vogelstein (Johns Hopkins University, Baltimore, Maryland) for kindly providing the HCT116 p53- and p21-$^{+/+}$ and $^{-/-}$ isogenic cell lines. We thank Justin Fishbaugh and Gene Hess at the Holden Comprehensive Cancer Center Flow Cytometry Facility for their expert technical assistance with the FACS analysis. We express our appreciation to Sarah Winckler and Jennifer L. Mannino for assistance with immunocytochemistry and Tina Samuels for antibody purification and testing. We thank Dr. Johannes W. Hell for discussion and a critical reading of the manuscript. This work was supported by NIH grant R01GM56900 and a Howard Hughes Medical Institute Pilot Grant to MCH.

References

1. Bennin DA, Don AS, Brake T, McKenzie JL, Rosenbaum H, Ortiz L, DePaoli-Roach AA, Horne MC. Cyclin G2 associates with protein phosphatase 2A catalytic and regulatory B' subunits in active complexes and induces nuclear aberrations and a G1/S phase cell cycle arrest. J Biol Chem 2002;277:27449–67. [PubMed: 11956189]
2. Noble ME, Endicott JA, Brown NR, Johnson LN. The cyclin box fold: protein recognition in cell-cycle and transcription control. Trends Biochem Sci 1997;22:482–7. [PubMed: 9433129]
3. Endicott JA, Noble ME. Structural principles in cell-cycle control: beyond the CDKs. Structure 1998;6:535–41. [PubMed: 9634691]
4. Nikolic M, Dudek H, Kwon YT, Ramos YF, Tsai LH. The cdk5/p35 kinase is essential for neurite outgrowth during neuronal differentiation. Genes Dev 1996;10:816–25. [PubMed: 8846918]
5. De Falco M, De Luca A. Involvement of cdks and cyclins in muscle differentiation. Eur J Histochem 2006;50:19–23. [PubMed: 16584981]
6. Loyer P, Trembley JH, Katona R, Kidd VJ, Lahti JM. Role of CDK/cyclin complexes in transcription and RNA splicing. Cell Signal 2005;17:1033–51. [PubMed: 15935619]
7. Horne MC, Goolsby GL, Donaldson KL, Tran D, Neubauer M, Wahl AF. Cyclin G1 and cyclin G2 comprise a new family of cyclins with contrasting tissue-specific and cell cycle-regulated expressions. Journal of Biological Chemistry 1996;271:6050–61. [PubMed: 8626390]
8. Horne MC, Donaldson KL, Goolsby GL, Tran D, Mulheisen M, Hell JW, Wahl AF. Cyclin G2 is up-regulated during growth inhibition and B cell antigen receptor-mediated cell cycle arrest. Journal of Biological Chemistry 1997;272:12650–61. [PubMed: 9139721]
9. Bates S, Rowan S, Vousden KH. Characterization of human cyclin G1 and G2: DNA damage inducible genes. Oncogene 1996;13:1103–1109. [PubMed: 8806701]
10. Gajate C, An F, Mollinedo F. Differential cytostatic and apoptotic effects of ecteinascidin-743 in cancer cells. Transcription-dependent cell cycle arrest and transcription-independent JNK and mitochondrial mediated apoptosis. J Biol Chem 2002;277:41580–9. [PubMed: 12198119]
11. Frasor J, Danes JM, Komm B, Chang KC, Lyttle CR, Katzenellenbogen BS. Profiling of estrogen up- and down-regulated gene expression in human breast cancer cells: insights into gene networks and pathways underlying estrogenic control of proliferation and cell phenotype. Endocrinology 2003;144:4562–74. [PubMed: 12959972]
12. Houldsworth J, Heath SC, Bosl GJ, Studer L, Chaganti RS. Expression profiling of lineage differentiation in pluripotential human embryonal carcinoma cells. Cell Growth Differ 2002;13:257–64. [PubMed: 12114215]
13. Oliver TG, Grasfeder LL, Carroll AL, Kaiser C, Gillingham CL, Lin SM, Wickramasinghe R, Scott MP, Wechsler-Reya RJ. Transcriptional profiling of the Sonic hedgehog response: a critical role for N-myc in proliferation of neuronal precursors. Proc Natl Acad Sci U S A 2003;100:7331–6. [PubMed: 12777630]
14. Ito Y, Yoshida H, Uruno T, Nakano K, Takamura Y, Miya A, Kobayashi K, Yokozawa T, Matsuzuka F, Kuma K, Miyauchi A. Decreased expression of cyclin G2 is significantly linked to the malignant transformation of papillary carcinoma of the thyroid. Anticancer Res 2003;23:2335–8. [PubMed: 12894512]

15. Murray JI, Whitfield ML, Trinklein ND, Myers RM, Brown PO, Botstein D. Diverse and specific gene expression responses to stresses in cultured human cells. Mol Biol Cell. 2004

16. Kim Y, Shintani S, Kohno Y, Zhang R, Wong DT. Cyclin G2 dysregulation in human oral cancer. Cancer Res 2004;64:8980–6. [PubMed: 15604262]

17. Martinez-Gac L, Marques M, Garcia Z, Campanero MR, Carrera AC. Control of Cyclin G2 mRNA Expression by Forkhead Transcription Factors: Novel Mechanism for Cell Cycle Control by Phosphoinositide 3-Kinase and Forkhead. Mol Cell Biol 2004;24:2181–2189. [PubMed: 14966295]

18. Burgering BM, Kops GJ. Cell cycle and death control: long live Forkheads. Trends Biochem Sci 2002;27:352–60. [PubMed: 12114024]

19. Okamoto K, Beach D. Cyclin G is a transcriptional target of the p53 tumor suppressor protein. EMBO Journal 1994;13:4816–22. [PubMed: 7957050]

20. Zauberman A, Lupo A, Oren M. Identification of p53 target genes through immune selection of genomic DNA: the cyclin G gene contains two distinct p53 binding sites. Oncogene 1995;10:2361–6. [PubMed: 7784084]

21. Jensen MR, Audolfsson T, Keck CL, Zimonjic DB, Thorgeirsson SS. Gene structure and chromosomal localization of mouse cyclin G2 (Ccng2). Gene 1999;230:171–80. [PubMed: 10216255]

22. Zhao L, Samuels T, Winckler S, Korgaonkar C, Tompkins V, Horne MC, Quelle DE. Cyclin G1 has growth inhibitory activity linked to the ARF-Mdm2-p53 and pRb tumor suppressor pathways. Mol Cancer Res 2003;1:195–206. [PubMed: 12556559]

23. Kimura SH, Nojima H. Cyclin G1 associates with MDM2 and regulates accumulation and degradation of p53 protein. Genes Cells 2002;7:869–80. [PubMed: 12167164]

24. Janssens V, Goris J. Protein phosphatase 2A: a highly regulated family of serine/threonine phosphatases implicated in cell growth and signalling. Biochemical Journal 2001;353:417–39. [PubMed: 11171037]

25. McCright B, Rivers AM, Audlin S, Virshup DM. The B56 family of protein phosphatase 2A (PP2A) regulatory subunits encodes differentiation-induced phosphoproteins that target PP2A to both nucleus and cytoplasm. J Biol Chem 1996;271:22081–9. [PubMed: 8703017]

26. Sontag E, Nunbhakdi-Craig V, Bloom GS, Mumby MC. A novel pool of protein phosphatase 2A is associated with microtubules and is regulated during the cell cycle. Journal of Cell Biology 1995;128:1131–44. [PubMed: 7896877]

27. Zhao Y, Boguslawski G, Zitomer RS, DePaoli-Roach AA. Saccharomyces cerevisiae homologs of mammalian B and B' subunits of protein phosphatase 2A direct the enzyme to distinct cellular functions. J Biol Chem 1997;272:8256–62. [PubMed: 9079645]

28. Sontag E, Nunbhakdi-Craig V, Lee G, Brandt R, Kamibayashi C, Kuret J, White CL III, Mumby MC, Bloom GS. Molecular interaction among protein phosphatase 2A, tau, and microtubules. J Biol Chem 1999;274:25490–25498. [PubMed: 10464280]

29. Takahashi M, Shibata H, Shimakawa M, Miyamoto M, Mukai H, Ono Y. Characterization of a novel giant scaffolding protein, CG-NAP, that anchors multiple signaling enzymes to centrosome and the golgi apparatus. Journal of Biological Chemistry 1999;274:17267–74. [PubMed: 10358086]

30. Cheng A, Balczon R, Zuo Z, Koons JS, Walsh AH, Honkanen RE. Fostriecin-mediated G2-M-phase growth arrest correlates with abnormal centrosome replication, the formation of aberrant mitotic spindles, and the inhibition of serine/threonine protein phosphatase activity. Cancer Research 1998;58:3611–9. [PubMed: 9721869]

31. Snaith HA, Armstrong CG, Guo Y, Kaiser K, Cohen PTW. Deficiency of protein phosphatase 2A uncouples the nuclear and centrosome cycles and prevents attachment of microtubules to the kinetochore in Drosophila microtubule star (mts) embryos. Journal of Cell Science 1996;109:3001–3012. [PubMed: 9004035]

32. Murphy MB, Levi SK, Egelhoff TT. Molecular characterization and immunolocalization of Dictyostelium discoideum protein phosphatase 2A. FEBS Lett 1999;456:7–12. [PubMed: 10452519]

33. Le Goff X, Buvelot S, Salimova E, Guerry F, Schmidt S, Cueille N, Cano E, Simanis V. The protein phosphatase 2A B'-regulatory subunit par1p is implicated in regulation of the S. pombe septation initiation network. FEBS Lett 2001;508:136–42. [PubMed: 11707284]

34. Jiang W, Hallberg RL. Isolation and characterization of par1(+) and par2(+): two Schizosaccharomyces pombe genes encoding B' subunits of protein phosphatase 2A. Genetics 2000;154:1025–38. [PubMed: 10757751]
35. Dobbelaere J, Gentry MS, Hallberg RL, Barral Y. Phosphorylation-dependent regulation of septin dynamics during the cell cycle. Dev Cell 2003;4:345–57. [PubMed: 12636916]
36. Gentry MS, Hallberg RL. Localization of Saccharomyces cerevisiae protein phosphatase 2A subunits throughout mitotic cell cycle. Mol Biol Cell 2002;13:3477–92. [PubMed: 12388751]
37. Doxsey S. Re-evaluating centrosome function. Nature Reviews Molecular Cell Biology 2001;2:688–98.
38. Hinchcliffe EH, Sluder G. "It takes two to tango": understanding how centrosome duplication is regulated throughout the cell cycle. Genes & Development 2001;15:1167–81. [PubMed: 11358861]
39. Bornens M. Centrosome composition and microtubule anchoring mechanisms. Current Opinion in Cell Biology 2002;14:25–34. [PubMed: 11792541]
40. Lange BMH. Integration of the centrosome in cell cycle control, stress response and signal transduction pathways. Current Opinion in Cell Biology 2002;14:35–43. [PubMed: 11792542]
41. Lacey KR, Jackson PK, Stearns T. Cyclin-dependent kinase control of centrosome duplication. Proceedings of the National Academy of Sciences of the United States of America 1999;96:2817–22. [PubMed: 10077594]
42. Matsumoto Y, Hayashi K, Nishida E. Cyclin-dependent kinase 2 (Cdk2) is required for centrosome duplication in mammalian cells. Current Biology 1999;9:429–32. [PubMed: 10226033]
43. Meraldi P, Lukas J, Fry AM, Bartek J, Nigg EA. Centrosome duplication in mammalian somatic cells requires E2F and Cdk2-cyclin A. Nature Cell Biology 1999;1:88–93.
44. Khodjakov A, Rieder CL. Centrosomes enhance the fidelity of cytokinesis in vertebrates and are required for cell cycle progression. Journal of Cell Biology 2001;153:237–42. [PubMed: 11285289]
45. Piel M, Nordberg J, Euteneuer U, Bornens M. Centrosome-dependent exit of cytokinesis in animal cells. [see comments]. Science 2001;291:1550–3. [PubMed: 11222861]
46. Sibon OC, Kelkar A, Lemstra W, Theurkauf WE. DNA-replication/DNA-damage-dependent centrosome inactivation in Drosophila embryos. Nat Cell Biol 2000;2:90–5. [PubMed: 10655588]
47. Lingle WL, Salisbury JL. The role of the centrosome in the development of malignant tumors. Curr Top Dev Biol 2000;49:313–29. [PubMed: 11005025]
48. Pihan GA, Purohit A, Wallace J, Malhotra R, Liotta L, Doxsey SJ. Centrosome defects can account for cellular and genetic changes that characterize prostate cancer progression. Cancer Research 2001;61:2212–9. [PubMed: 11280789]
49. Lingle WL, Barrett SL, Negron VC, D'Assoro AB, Boeneman K, Liu W, Whitehead CM, Reynolds C, Salisbury JL. Centrosome amplification drives chromosomal instability in breast tumor development. Proc Natl Acad Sci U S A 2002;99:1978–83. [PubMed: 11830638]
50. Nigg EA. Centrosome aberrations: cause or consequence of cancer progression? Nat Rev Cancer 2002;2:815–25. [PubMed: 12415252]
51. D'Assoro AB, Lingle WL, Salisbury JL. Centrosome amplification and the development of cancer. Oncogene 2002;21:6146–53. [PubMed: 12214243]
52. Hall DD, Feekes JA, Arachchige Don AS, Shi M, Hamid J, Chen L, Strack S, Zamponi GW, Horne MC, Hell JW. Binding of protein phosphatase 2A to the L-type calcium channel Cav1.2 next to Ser1928, its main PKA site, is critical for Ser1928 dephosphorylation. Biochemistry 2006;45:3448–59. [PubMed: 16519540]
53. Bunz F, Dutriaux A, Lengauer C, Waldman T, Zhou S, Brown JP, Sedivy JM, Kinzler KW, Vogelstein B. Requirement for p53 and p21 to sustain G2 arrest after DNA damage. Science 1998;282:1497–501. [PubMed: 9822382]
54. Gillingham AK, Munro S. The PACT domain, a conserved centrosomal targeting motif in the coiled-coil proteins AKAP450 and pericentrin. EMBO Reports 2000;1:524–9. [PubMed: 11263498]
55. White RA, Pan Z, Salisbury JL. GFP-centrin as a marker for centriole dynamics in living cells. Microscopy Research & Technique 2000;49:451–7. [PubMed: 10842372]

56. Jordan M, Schallhorn A, Wurm FM. Transfecting mammalian cells: optimization of critical parameters affecting calcium-phosphate precipitate formation. Nucleic Acids Res 1996;24:596–601. [PubMed: 8604299]
57. Wadzinski BE, Eisfelder BJ, Peruski LF Jr, Mumby MC, Johnson GL. NH2-terminal modification of the phosphatase 2A catalytic subunit allows functional expression in mammalian cells. J Biol Chem 1992;267:16883–8. [PubMed: 1380955]
58. Vallee RB, Collins CA. Purification of microtubules and microtubule-associated proteins from sea urchin eggs and cultured mammalian cells using taxol, and use of exogenous taxol-stabilized brain microtubules for purifying microtubule-associated proteins. Methods Enzymol 1986;134:116–27. [PubMed: 2881189]
59. Vallee RB. Purification of brain microtubules and microtubule-associated protein 1 using taxol. Methods Enzymol 1986;134:104–15. [PubMed: 2881188]
60. Solomon F. Direct identification of microtubule-associated proteins by selective extraction of cultured cells. Meth Enzymol 1986;134:139–147. [PubMed: 3821557]
61. Moudjou, M.; Bornens, M. Method of centrosome isolation from cultured animal cells. In: Celis, JE., editor. Cell Biology: A Laboratory Handbook. 2. Academic Press; London: 1998.
62. Paoletti A, Moudjou M, Paintrand M, Salisbury JL, Bornens M. Most of centrin in animal cells is not centrosome-associated and centrosomal centrin is confined to the distal lumen of centrioles. J Cell Sci 1996;109 (Pt 13):3089–102. [PubMed: 9004043]
63. Balczon, R. Methods for the Study of Centrosome Reproduction in Mammalian Cells. In: Palazzo, RE.; Davis, TN., editors. Centrosomes and Spindle Pole Bodies. Academic Press; San Diego: 2001.
64. Bornens, M.; Moudjou, M. Studying the Composition and Function of Centrosomes in Vertebrates. In: Reider, CL., editor. Mitosis and Meiosis. Academic Press; San Diego: 1999.
65. Hirokawa N. Microtubule organization and dynamics dependent on microtubule-associated proteins. Curr Opin Cell Biol 1994;6:74–81. [PubMed: 8167029]
66. Andersen SS. Spindle assembly and the art of regulating microtubule dynamics by MAPs and Stathmin/Op18. Trends Cell Biol 2000;10:261–7. [PubMed: 10856928]
67. Moudjou M, Paintrand M, Vigues B, Bornens M. A human centrosomal protein is immunologically related to basal body-associated proteins from lower eucaryotes and is involved in the nucleation of microtubules. J Cell Biol 1991;115:129–40. [PubMed: 1918132]
68. Moudjou M, Bordes N, Paintrand M, Bornens M. gamma-Tubulin in mammalian cells: the centrosomal and the cytosolic forms. J Cell Sci 1996;109 (Pt 4):875–87. [PubMed: 8718679]
69. Hannus M, Feiguin F, Heisenberg CP, Eaton S. Planar cell polarization requires Widerborst, a B' regulatory subunit of protein phosphatase 2A. Development 2002;129:3493–3503. [PubMed: 12091318]
70. Wong C, Stearns T. Centrosome number is controlled by a centrosome-intrinsic block to reduplication. Nat Cell Biol 2003;5:539–44. [PubMed: 12766773]
71. Liu X, Erikson RL. Activation of Cdc2/cyclin B and inhibition of centrosome amplification in cells depleted of Plk1 by siRNA. Proc Natl Acad Sci U S A 2002;99:8672–6. [PubMed: 12077309]
72. Louie RK, Bahmanyar S, Siemers KA, Votin V, Chang P, Stearns T, Nelson WJ, Barth AI. Adenomatous polyposis coli and EB1 localize in close proximity of the mother centriole and EB1 is a functional component of centrosomes. J Cell Sci 2004;117:1117–28. [PubMed: 14970257]
73. Andersen JS, Wilkinson CJ, Mayor T, Mortensen P, Nigg EA, Mann M. Proteomic characterization of the human centrosome by protein correlation profiling. Nature 2003;426:570–4. [PubMed: 14654843]
74. Keryer G, Witczak O, Delouvee A, Kemmner WA, Rouillard D, Tasken K, Bornens M. Dissociating the Centrosomal Matrix Protein AKAP450 from Centrioles Impairs Centriole Duplication and Cell Cycle Progression. Mol Biol Cell 2003;14:2436–46. [PubMed: 12808041]
75. Salisbury JL, Suino KM, Busby R, Springett M. Centrin-2 is required for centriole duplication in mammalian cells. Curr Biol 2002;12:1287–92. [PubMed: 12176356]
76. Piel M, Meyer P, Khodjakov A, Rieder CL, Bornens M. The respective contributions of the mother and daughter centrioles to centrosome activity and behavior in vertebrate cells. J Cell Biol 2000;149:317–30. [PubMed: 10769025]

77. Moritz M, Agard DA. Gamma-tubulin complexes and microtubule nucleation. Curr Opin Struct Biol 2001;11:174–81. [PubMed: 11297925]

78. Schmidt PH, Dransfield DT, Claudio JO, Hawley RG, Trotter KW, Milgram SL, Goldenring JR. AKAP350, a multiply spliced protein kinase A-anchoring protein associated with centrosomes. J Biol Chem 1999;274:3055–66. [PubMed: 9915845]

79. Witczak O, Skalhegg BS, Keryer G, Bornens M, Tasken K, Jahnsen T, Orstavik S. Cloning and characterization of a cDNA encoding an A-kinase anchoring protein located in the centrosome, AKAP450. Embo J 1999;18:1858–68. [PubMed: 10202149]

80. Sillibourne JE, Milne DM, Takahashi M, Ono Y, Meek DW. Centrosomal anchoring of the protein kinase CK1delta mediated by attachment to the large, coiled-coil scaffolding protein CG-NAP/AKAP450. J Mol Biol 2002;322:785–97. [PubMed: 12270714]

81. Wang Y, Burke DJ. Cdc55p, the B-type regulatory subunit of protein phosphatase 2A, has multiple functions in mitosis and is required for the kinetochore/spindle checkpoint in Saccharomyces cerevisiae. Mol Cell Biol 1997;17:620–6. [PubMed: 9001215]

82. Wera S, Fernandez A, Lamb NJ, Turowski P, Hemmings-Mieszczak M, Mayer-Jaekel RE, Hemmings BA. Deregulation of translational control of the 65-kDa regulatory subunit (PR65 alpha) of protein phosphatase 2A leads to multinucleated cells. J Biol Chem 1995;270:21374–81. [PubMed: 7673173]

83. Mayer-Jaekel RE, Ohkura H, Gomes R, Sunkel CE, Baumgartner S, Hemmings BA, Glover DM. The 55 kd regulatory subunit of Drosophila protein phosphatase 2A is required for anaphase. Cell 1993;72:621–33. [PubMed: 8382567]

84. Kinoshita N, Yamano H, Niwa H, Yoshida T, Yanagida M. Negative regulation of mitosis by the fission yeast protein phosphatase ppa2. Genes Dev 1993;7:1059–71. [PubMed: 8389306]

85. Gurland G, Gundersen GG. Stable, detyrosinated microtubules function to localize vimentin intermediate filaments in fibroblasts. J Cell Biol 1995;131:1275–90. [PubMed: 8522589]

86. Sontag E, Nunbhakdi-Craig V, Lee G, Bloom GS, Mumby MC. Regulation of the phosphorylation state and microtubule-binding activity of Tau by protein phosphatase 2A. Neuron 1996;17:1201–1207. [PubMed: 8982166]

87. Kaltschmidt JA, Brand AH. Asymmetric cell division: microtubule dynamics and spindle asymmetry. J Cell Sci 2002;115:2257–64. [PubMed: 12006610]

88. Wu X, Xiang X, Hammer JA 3rd. Motor proteins at the microtubule plus-end. Trends Cell Biol 2006;16:135–43. [PubMed: 16469495]

89. Vaughan KT. TIP maker and TIP marker; EB1 as a master controller of microtubule plus ends. J Cell Biol 2005;171:197–200. [PubMed: 16247021]

90. Tighe A, Johnson VL, Albertella M, Taylor SS. Aneuploid colon cancer cells have a robust spindle checkpoint. EMBO Rep 2001;2:609–14. [PubMed: 11454737]

91. van Es JH, Giles RH, Clevers HC. The many faces of the tumor suppressor gene APC. Exp Cell Res 2001;264:126–34. [PubMed: 11237529]

92. Rosa J, Canovas P, Islam A, Altieri DC, Doxsey SJ. Survivin modulates microtubule dynamics and nucleation throughout the cell cycle. Mol Biol Cell 2006;17:1483–93. [PubMed: 16407408]

93. Fortugno P, Wall NR, Giodini A, O'Connor DS, Plescia J, Padgett KM, Tognin S, Marchisio PC, Altieri DC. Survivin exists in immunochemically distinct subcellular pools and is involved in spindle microtubule function. J Cell Sci 2002;115:575–85. [PubMed: 11861764]

94. Mack G, Rattner JB. Centrosome repositioning immediately following karyokinesis and prior to cytokinesis. Cell Motil Cytoskeleton 1993;26:239–47. [PubMed: 8293479]

95. Mogensen MM, Malik A, Piel M, Bouckson-Castaing V, Bornens M. Microtubule minus-end anchorage at centrosomal and non-centrosomal sites: the role of ninein. J Cell Sci 2000;113:3013–23. [PubMed: 10934040]

96. Chevrier V, Piel M, Collomb N, Saoudi Y, Frank R, Paintrand M, Narumiya S, Bornens M, Job D. The Rho-associated protein kinase p160ROCK is required for centrosome positioning. J Cell Biol 2002;157:807–17. [PubMed: 12034773]

97. Ou YY, Rattner JB. Post-karyokinesis centrosome movement leaves a trail of unanswered questions. Cell Motil Cytoskeleton 2002;51:123–32. [PubMed: 11921169]

98. Meraldi P, Honda R, Nigg EA. Aurora-A overexpression reveals tetraploidization as a major route to centrosome amplification in p53−/− cells. Embo J 2002;21:483–92. [PubMed: 11847097]

99. Andreassen PR, Lohez OD, Lacroix FB, Margolis RL. Tetraploid state induces p53-dependent arrest of nontransformed mammalian cells in G1. Molecular Biology of the Cell 2001;12:1315–28. [PubMed: 11359924]

100. Gromley A, Jurczyk A, Sillibourne J, Halilovic E, Mogensen M, Groisman I, Blomberg M, Doxsey S. A novel human protein of the maternal centriole is required for the final stages of cytokinesis and entry into S phase. J Cell Biol 2003;161:535–45. [PubMed: 12732615]

101. Borel F, Lohez OD, Lacroix FB, Margolis RL. Multiple centrosomes arise from tetraploidy checkpoint failure and mitotic centrosome clusters in p53 and RB pocket protein-compromised cells. Proc Natl Acad Sci U S A 2002;99:9819–24. [PubMed: 12119403]

102. Tarapore P, Fukasawa K. Loss of p53 and centrosome hyperamplification. Oncogene 2002;21:6234–40. [PubMed: 12214254]

103. Hinchcliffe EH, Miller FJ, Cham M, Khodjakov A, Sluder G. Requirement of a centrosomal activity for cell cycle progression through G1 into S phase. [see comments]. Science 2001;291:1547–50. [PubMed: 11222860]

104. La Terra S, English CN, Hergert P, McEwen BF, Sluder G, Khodjakov A. The de novo centriole assembly pathway in HeLa cells: cell cycle progression and centriole assembly/maturation. J Cell Biol 2005;168:713–22. [PubMed: 15738265]

105. Keryer G, Di Fiore B, Celati C, Lechtreck KF, Mogensen M, Delouvee A, Lavia P, Bornens M, Tassin AM. Part of Ran is associated with AKAP450 at the centrosome: involvement in microtubule-organizing activity. Mol Biol Cell 2003;14:4260–71. [PubMed: 14517334]

106. Forgues M, Difilippantonio MJ, Linke SP, Ried T, Nagashima K, Feden J, Valerie K, Fukasawa K, Wang XW. Involvement of Crm1 in hepatitis B virus X protein-induced aberrant centriole replication and abnormal mitotic spindles. Mol Cell Biol 2003;23:5282–92. [PubMed: 12861014]

107. Di Fiore B, Ciciarello M, Mangiacasale R, Palena A, Tassin AM, Cundari E, Lavia P. Mammalian RanBP1 regulates centrosome cohesion during mitosis. J Cell Sci 2003;116:3399–411. [PubMed: 12840069]

108. Di Fiore B, Ciciarello M, Lavia P. Mitotic Functions of the Ran GTPase Network: The Importance of Being in the Right Place at the Right Time. Cell Cycle 2004;3

ABBREVIATIONS

DC
daughter centriole

ECL
enhanced chemiluminescence

FITC
fluorescein isothiocyanate

GFP
green fluorescent protein

GST
glutathione S-transferase

HRP
horseradish peroxidase

HU
hydroxyurea

LRSC
lissamine rhodamine sulfonyl chloride

MT

microtubule

MTOC
microtubule organizing center

APC
adenomatous polyposis coli

MC
mother centriole

AKAPs
protein kinase A-anchoring proteins

PBS
phosphate-buffered saline

PCM
pericentriolar material

PCR
polymerase chain reaction

SDS-PAGE
SDS-polyacrylamide gel electrophoresis

TBS
Tris-buffered saline

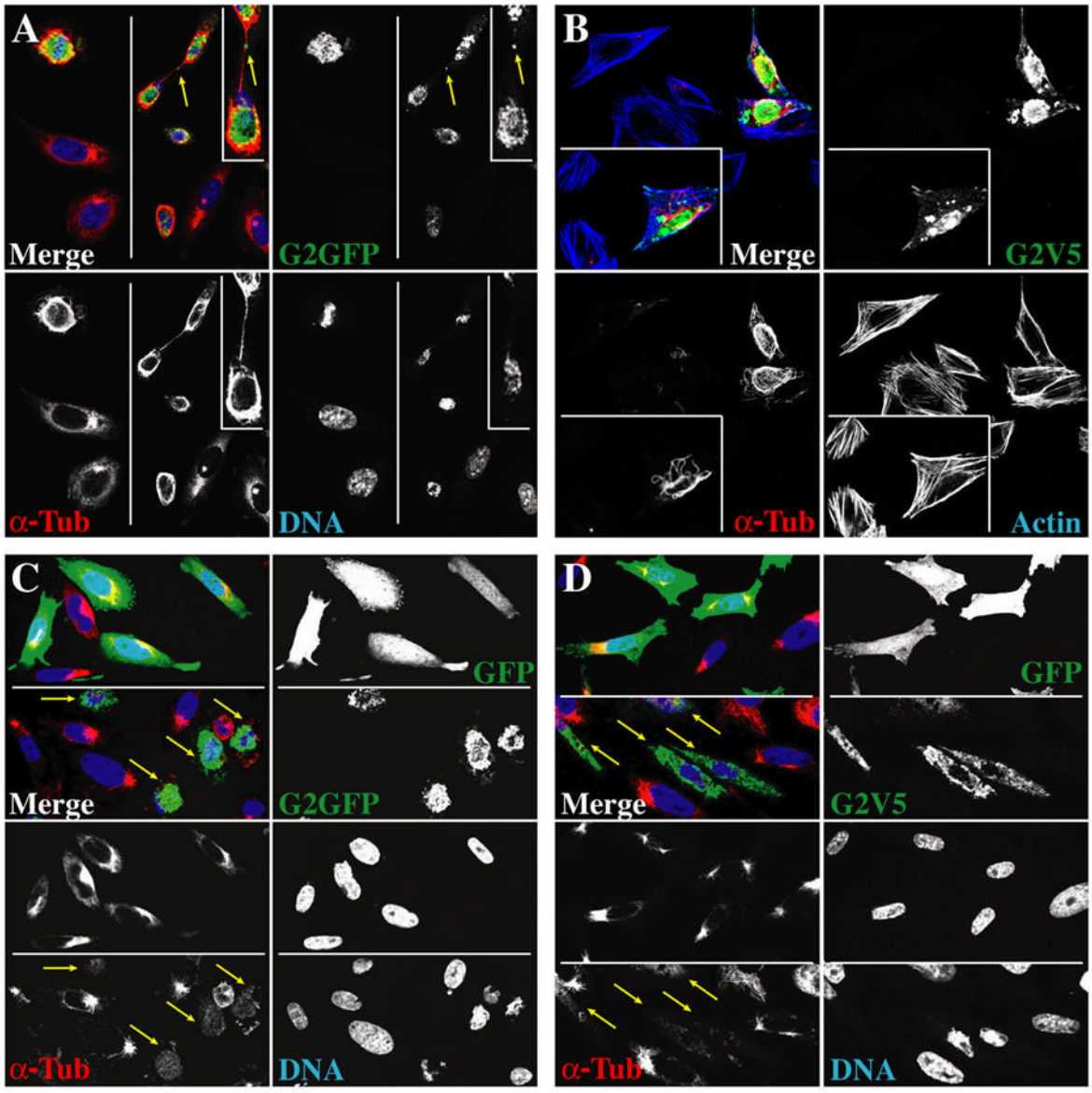

Fig. 1. High-level ectopic cyclin G2 expression alters microtubule stability

(A–D) Micrograph images of 0.3 μM optical sections of CHO cells transfected with pcDNA3 expression constructs encoding G2-GFP (A, C top panel, lower right), G2V5His (B, D top panel, lower right), or GFP alone (C, D top panels, upper right) obtained by confocal immunofluorescence microscopy. (A) Control cells and those expressing cyclin G2-GFP were treated with 1 μM nocodazole for 15 minutes followed by washout and a three-minute release into drug free medium prior to fixation with 4% paraformaldehyde. Nuclear DNA was stained with TOTO-3 and MTs in fixed cells were labeled with the DM1A mouse anti-α-tubulin antibody. Images collected from two different fields of the same slide are shown on left and right. The arrow indicates a bright dot of cyclin G2 associated with the mid-zone MT-bridge of cells undergoing cytokinesis. The inset shows a larger magnification of this region. (B) Cells expressing cyclin G2-V5His were treated with nocodazole for 30 minutes, pre-extracted with Triton X-100 in PHEM buffer, rinsed and fixed with methanol. F-Actin is detected with fluorescently labeled phalloidin. The inset shows cells from another field of the same slide.

(C, D) Cultures were transfected with cyclin G2-GFP (C, bottom field in each top panel), G2V5His (D, bottom field in each top panel) or GFP (C, D, top fields) and treated for 2 hours with nocodazole, followed by rinse and release into drug-free medium for 3 minutes, and then fixed with paraformaldehyde. Cyclin G2V5His was detected with rabbit anti-cyclin G2 antibody (green), followed by FITC-conjugated donkey anti-rabbit IgG. DNA (right fields in each bottom panel) and MTs (left fields in each bottom panel) were stained as above. Immuno-signals are shown pseudo colored in the merged panels as indicated by the font color of the single channel labels. Single channel signals are shown in black and white for better contrast.

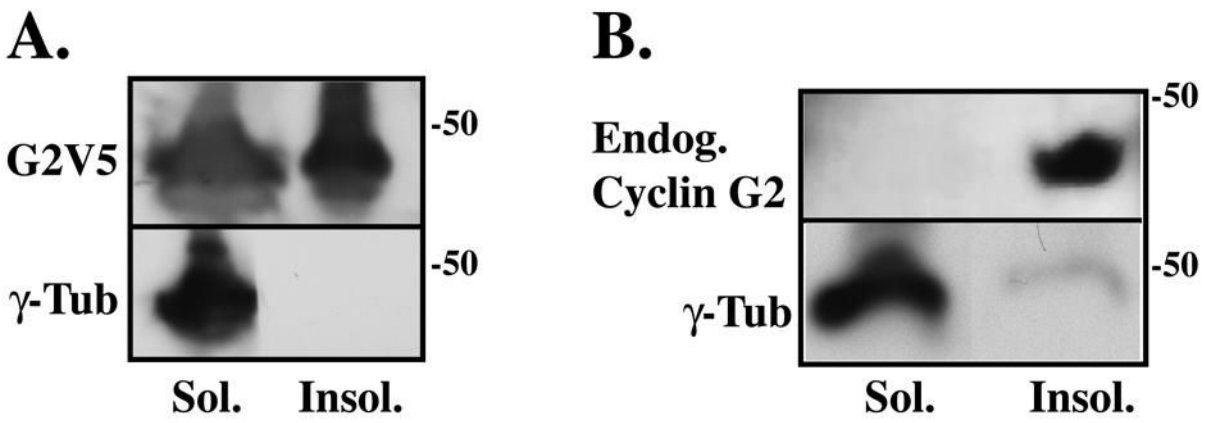

Fig. 2. Endogenous and ectopic cyclin G2 distributes to detergent-resistant insoluble protein fractions

(A, B) Immunoblot analysis of soluble (Sol.) and insoluble (Insol.) proteins fractionated from cyclin G2V5His transfected (A) and nontransfected (B) U2OS cells. Cells were harvested, washed in PBS, and lysed in PHEM buffer containing 1% Triton X-100. A low speed 300 g centrifugation step separated soluble proteins from the insoluble protein pellet. Soluble proteins present in the supernatant were precipitated with methanol and pelleted. The soluble and insoluble protein pellets were washed in PHEM buffer, solubilized in sample buffer and an equivalent volume of each fraction was loaded onto a SDS-PAGE gel. Immunoblot analysis using rabbit anti-cyclin G2 and mouse anti-γ-tubulin shows the distribution of ectopic G2V5 (A) and endogenous G2 (B) primarily in the detergent resistant insoluble fraction relative to γ-tubulin, which distributes to the soluble fraction.

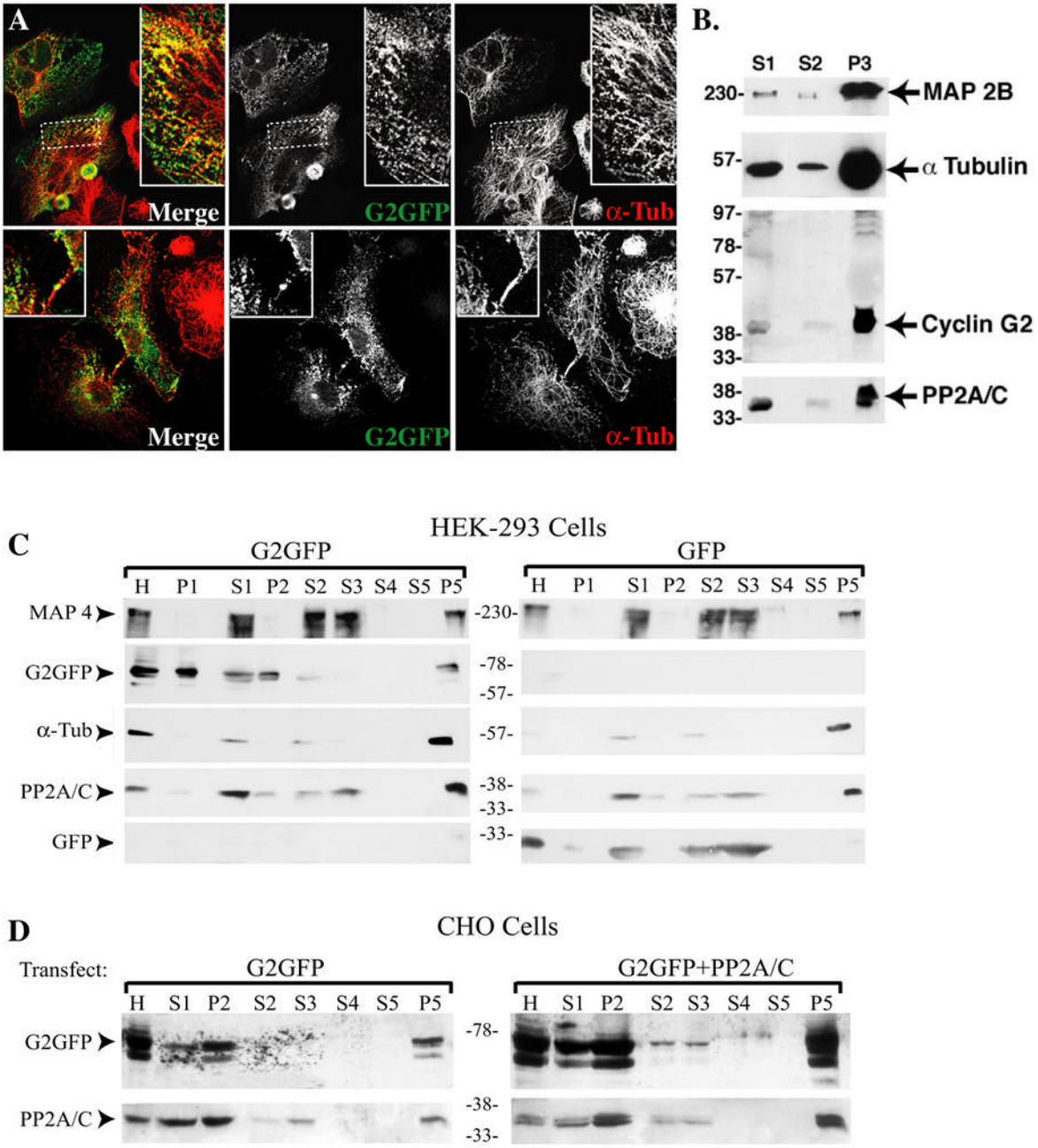

Fig. 3. Both endogenous and ectopic cyclin G2 associate and copurify with microtubules

(A) Confocal fluorescence microscopy optical section (0.3 μM) images of CHO (top panels) and COS-7 cells (bottom panels) expressing cyclin G2-GFP. Cultures were treated with nocodazole for 1.5 hours and either released for 10 minutes in drug free medium (top) or not released (bottom), pre-extracted in PHEM buffer containing 0.5 % Triton X-100, fixed in 4% paraformaldehyde, and labeled with DM1A anti-α-tubulin antibodies. (B) Immunoblots of the indicated proteins demonstrate copurification of endogenous cyclin G2 and PP2A/C with Paclitaxel-stabilized MTs isolated from rat brain tissue. Brain tissue was homogenized in PME buffer (0.1 M PIPES, pH 6.9, 1 mM $MgSO_4$, 2 mM EGTA, 1 mM DTT). Pelleted MTs were washed two times by resuspension in homogenization buffer containing 20 μM Paclitaxel

centrifugation through a 10% sucrose cushion. Samples loaded on gel include the low speed (S1, 30,000xg, 15 min; 20% of total fraction), high speed (S2, 180,000xg, 90 min; 20% of total) supernatants, and washed stabilized MT pellet (P3; 30% of total). (C&D) Copurification of ectopic cyclin G2 and PP2A/C with MTs isolated from transfected HEK293 (C) and CHO (D) cells. Samples from each transfection include the homogenate (H), and as above in *B*, the low speed (S1, 20% of total), and high speed (S2, 20% of total) supernatants and their respective pellets (P1 and P2; 10%), and the final stabilized MT pellets (P5; 50% of total remaining MTs after two washes; S3, S4, and S5 corresponding to the respective wash supernatants). All protein samples were fractionated by SDS-PAGE and immunoblotted with antibodies against the indicated proteins. Apparent molecular masses of standard marker proteins are depicted in kDa. The rabbit polyclonal antibody against cyclin G2 detects both endogenous cyclin G2 from rat brain as well as transfected G2-GFP from cell lines. Cyclin G2 and PP2A are associated with the assembled stabilized MTs (P3/P5; brain/cell lines, respectively).

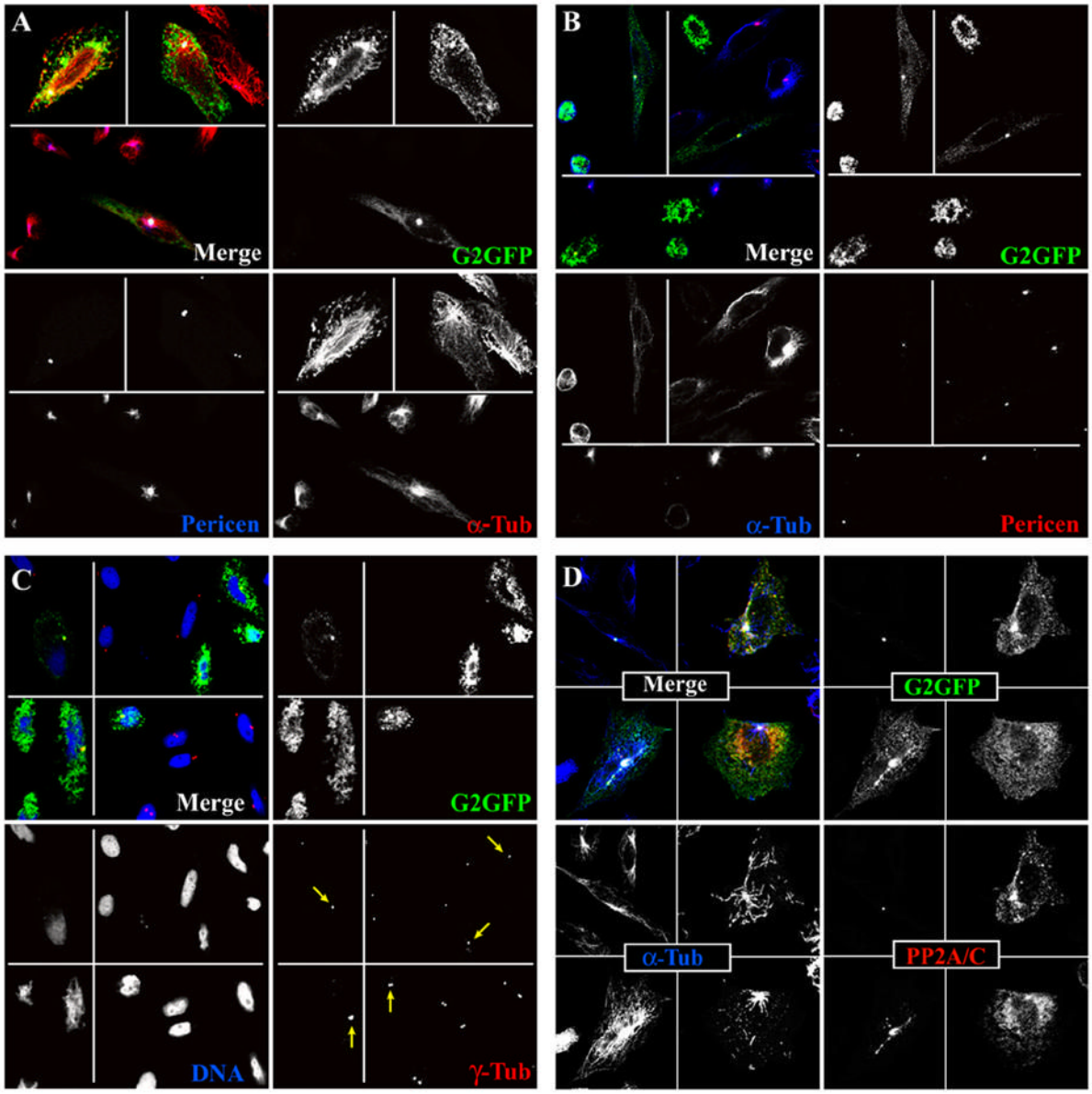

Fig. 4. Ectopic cyclin G2 colocalizes with PP2A/C at MTOCs/centrosomes in CHO cells

Optical section (0.3μM) images obtained by confocal immunofluorescence microscopy are shown. Immunosignals are shown pseudo-colored in the merge fields as indicated by the font color of the single channel labels. Single channel signals are shown in black and white for better contrast. (A) Transfected cultures were treated with nocodazole for 4 h and released into drug-free medium for a 10 min pulse (top fields in each panel) or drug treated for 30 min and released for a 3 min pulse (bottom fields) of MT regrowth prior to fixation. (B) Transfected cultures were treated with nocodazole for 2 h and released into drug-free media for a 30 min pulse (top fields in each panel) or for a 3 min pulse (bottom field) of MT regrowth prior to pre-extraction and paraformaldehyde fixation. MTs were labeled with DM1A anti-α-tubulin antibody (red in *A* and blue in *B*) and centrosomes with rabbit anti-pericentrin antibody (blue in *A* and red in *B*). (C) Cells were blocked with nocodazole (left panels for 40 min; right panels for 2 h). Cells in left panels were fixed immediately; those in the right panels were washed and released in drug-free media for 3 min prior to pre-extraction. All cells were fixed in MeOH.

Staining of coverslips with anti-γ tubulin and TOTO-3 revealed centrosomes (red) and DNA (blue), respectively. (D) Cells co-transfected with HA-PP2A/C and cyclin G2-GFP expression vectors were treated with nocodazole (upper panels 25 min, lower right panel 4 h) and released (upper panels 3.5 min, lower right panel 5 min) in drug-free media. Cells in the lower left panel were untreated. All cells were pre-extracted with 0.5% Triton X-100 and fixed with paraformaldehyde. MTs are probed with DM1A anti-α-tubulin (blue) and PP2A/C with sheep anti-PP2A/C (red).

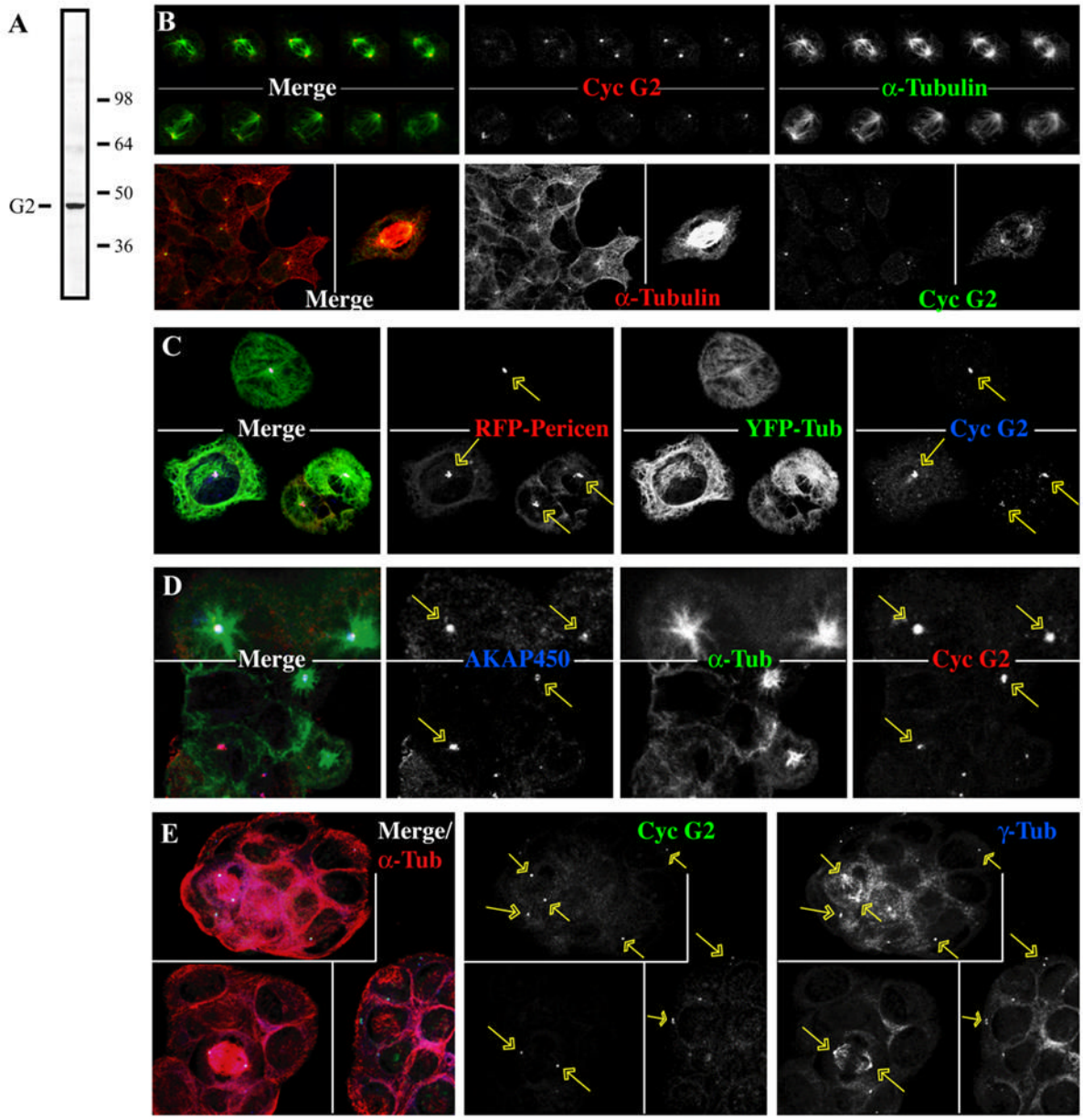

Fig. 5. Endogenous cyclin G2 localizes at centrosomes

(A) Immunoblot of U2OS cell lysate. Asynchronous, logarithmically growing cells were solubilized with RIPA buffer and blots probed with anti-cyclin G2 antibodies. Molecular mass markers are indicated on the right (in kDa) and the expected position of the 42 kDa cyclin G2 on the left. (B–E) Immunofluorescence confocal microscopy of U2OS and MCF-7 cells. Cyclin G2 was detected with antibodies as above. Immunofluorescence signals are pseudo-colored in the merge fields as indicated by the font color of the single channel shown in black and white. Arrows indicate the cyclin G2 positive centrosomes. (B) Top panels. Serial 0.3 μM confocal sections (top to bottom from left to right) of two different mitotic U2OS cells stained with rabbit anti-cyclin G2 (red) and anti-α-tubulin (green). Bottom panels. Interphase (left) and mitotic (right) U2OS cells are stained for MTs (red) and cyclin G2 (green). (C) U2OS cells expressing RFP-labeled pericentrin-PACT and YFP-labeled α-tubulin arrested in S-phase by

treatment with 4 mM HU for 48 hours to promote centrosome amplification and coalescence. Cells were fixed directly after treatment (top panels), or released from the S-phase block by incubation in 5 mM caffeine for 5 hours to allow the coalesced centrosomes to separate (bottom panels). (D) Nocodazole block (4h) and release (5 min) experiments of U2OS cells, MeOH fixed and immunostained with anti-AKAP450 antibody 14G2 (blue), rabbit anti-cyclin G2 (red), and DM1A anti-α-tubulin (green). (E) MCF-7 cells immunostained with mouse anti-γ-tubulin (blue), rabbit anti-cyclin G2 (green) and sheep anti-α-tubulin (red).

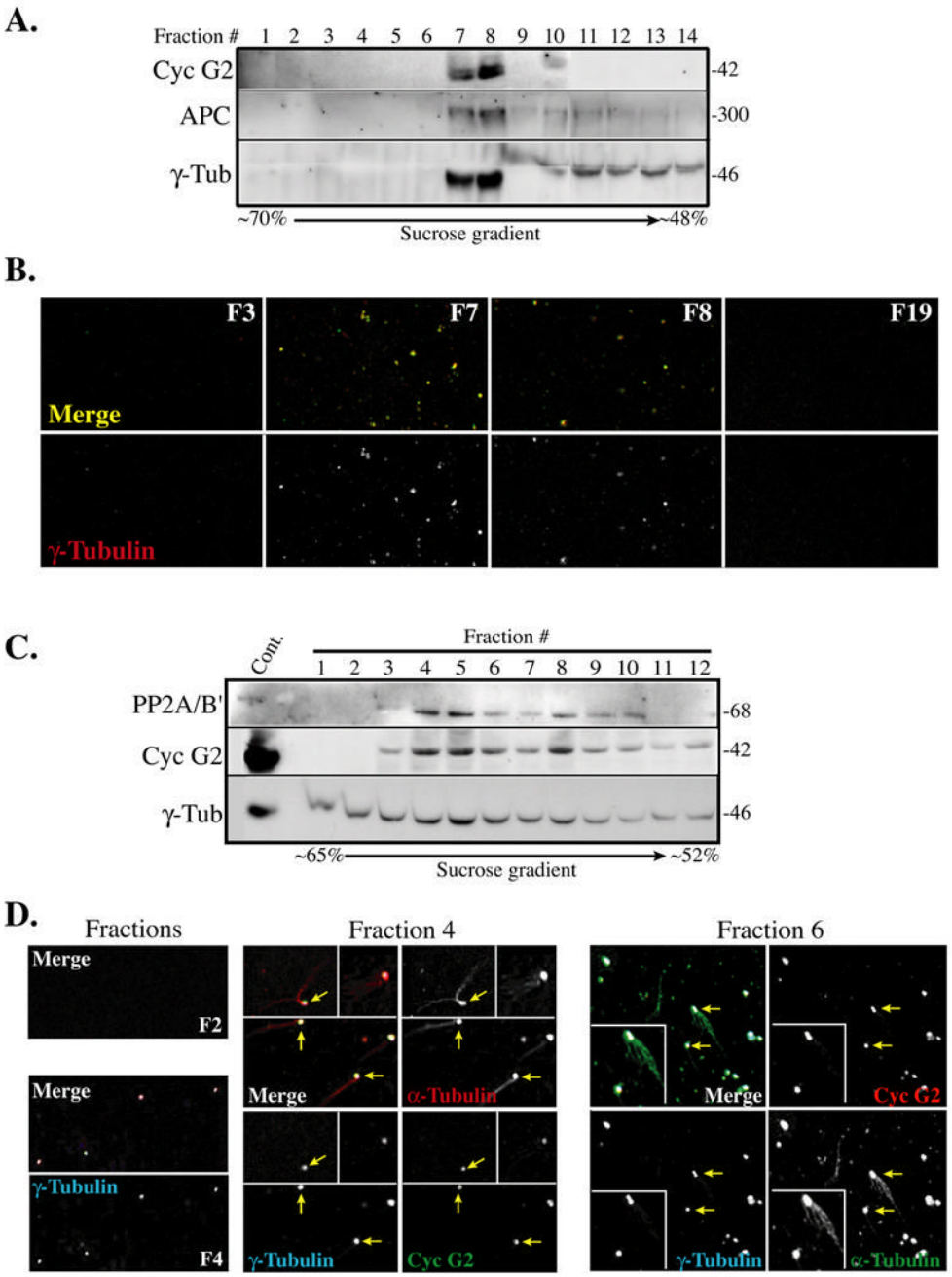

Fig. 6. Endogenous cyclin G2 and PP2A co-purify with centrosomes

Centrosomes were enriched from asynchronously growing log-phase U2OS cell cultures by subcellular fractionation and discontinuous sucrose gradient centrifugation as described by Bornens and Moudjou [61,64]. (A) Immunoblot analysis shows particulate material from sucrose gradient fractions (1–14), which was spun through a 1 ml buffer cushion. The arrow scale below the blot indicates the direction and the percentage of the sucrose gradient concentration. Cyclin G2 peaks and co-fractionates with the centrosomal marker γ-tubulin at the expected sucrose density for a centrosomal enriched fraction (~60%). Samples for fractions 9 and 10 were partially lost/migrated anomalously. (B) Representative immunofluorescence micrographs of 0.3 μM confocal optical sections of particulate material from indicated gradient

fractions (F3, F7, F8, and F19) from experiment shown in *A*. Samples were sedimented through a glycerol solution onto coverslips, treated with Triton X-100, fixed with methanol and immunostained for the indicated proteins. Bottom panels show anti-cyclin G2 staining of γ-tubulin positive particles in the two peak fractions (F7 and F8) shown in *A*; this staining pattern was absent from γ-tubulin negative fractions (F3 and F19). Top panels in *B* show merged images of optical sections from fluorescence channels corresponding to rabbit anti-cyclin G2 (green pseudo-color) and mouse anti-γ-tubulin (red). The resulting yellow color in the merge indicates anti-G2 and γ-tubulin co-staining of centrosomes. (C) Immunoblot analysis of the indicated proteins in fractions 1–12 collected from a ~65–52% sucrose gradient in a similar centrosome isolation experiment as described above in *A* with the exception that smaller volumes were collected per fraction in C. Note that fractions 4 through 6 show peak amounts of cyclin G2 and PP2A/B' co-fractionating with γ-tubulin at the expected position within the sucrose (~60 %) gradient. These observations were confirmed in two other experiments. (D) Confocal immunofluorescence microscopy images of *In vitro* microtubule nucleation assays performed using particulate material from fractions F2, F4, and F6 isolated from experiment depicted above in *C*. Prior to sedimentation of fraction aliquots onto coverslips, the material in each was incubated with purified α- and β-tubulin and GTP. Shown are merged images of 0.3 μM confocal optical sections obtained from rabbit anti-cyclin G2, mouse anti-γ-tubulin, and sheep anti-α-tubulin immunostained fractions (font color indicates pseudo-color of the corresponding channel signal in each RGB merge image). Yellow arrows indicate those MTs displaying clear asters. At left panels in *D* are representative images obtained from parallel MT nucleation assays done with fractioned material from F2 and F4. Note the lack of α–tubulin positive foci or MT arrays, or puncta co-staining with cyclin G2 or γ-tubulin antibodies in gradient samples from F2.

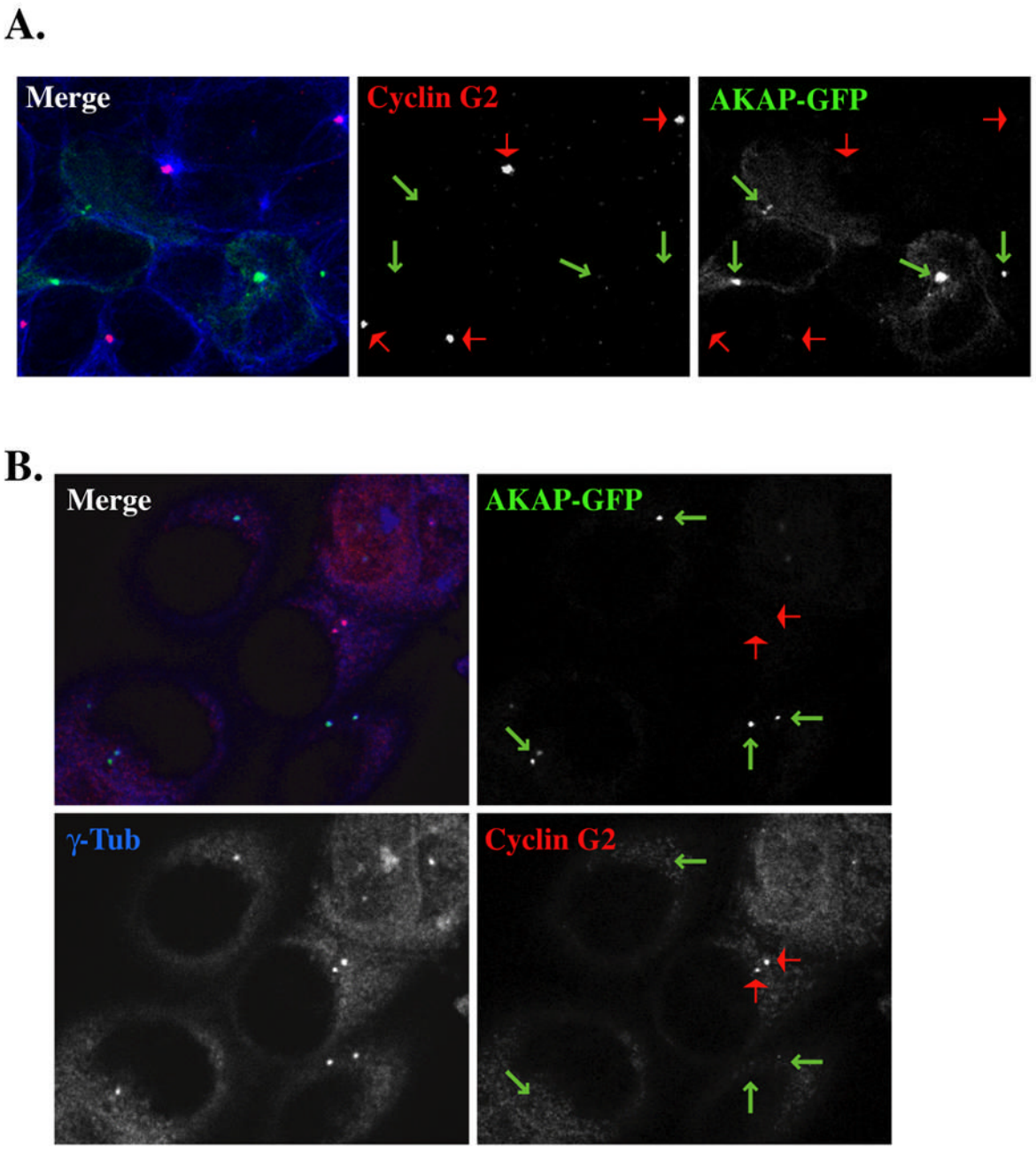

Fig. 7. Centrosomal localization of GFP-tagged AKAP450 C-terminus dissociates endogenous cyclin G2 from the centrosome

Micrographs of 0.3 μM optical sections from AKAP-GFP transfected U2OS (A) or MCF-7 (B) cells, fixed with MeOH, and immunostained with antibodies against cyclin G2 (red) in (A and B), and α- (in A) or (in B) γ-tublin (blue). Shown in merge fields are the pseudo-colored fluorescence signals of the single channels black and white. The arrows indicate the centrosomal localization of AKAP-GFP (green) and cyclin G2 (red). Note the absence of centrosomal cyclin G2 in cells expressing AKAP-GFP at MTOCs/ centrosomes.

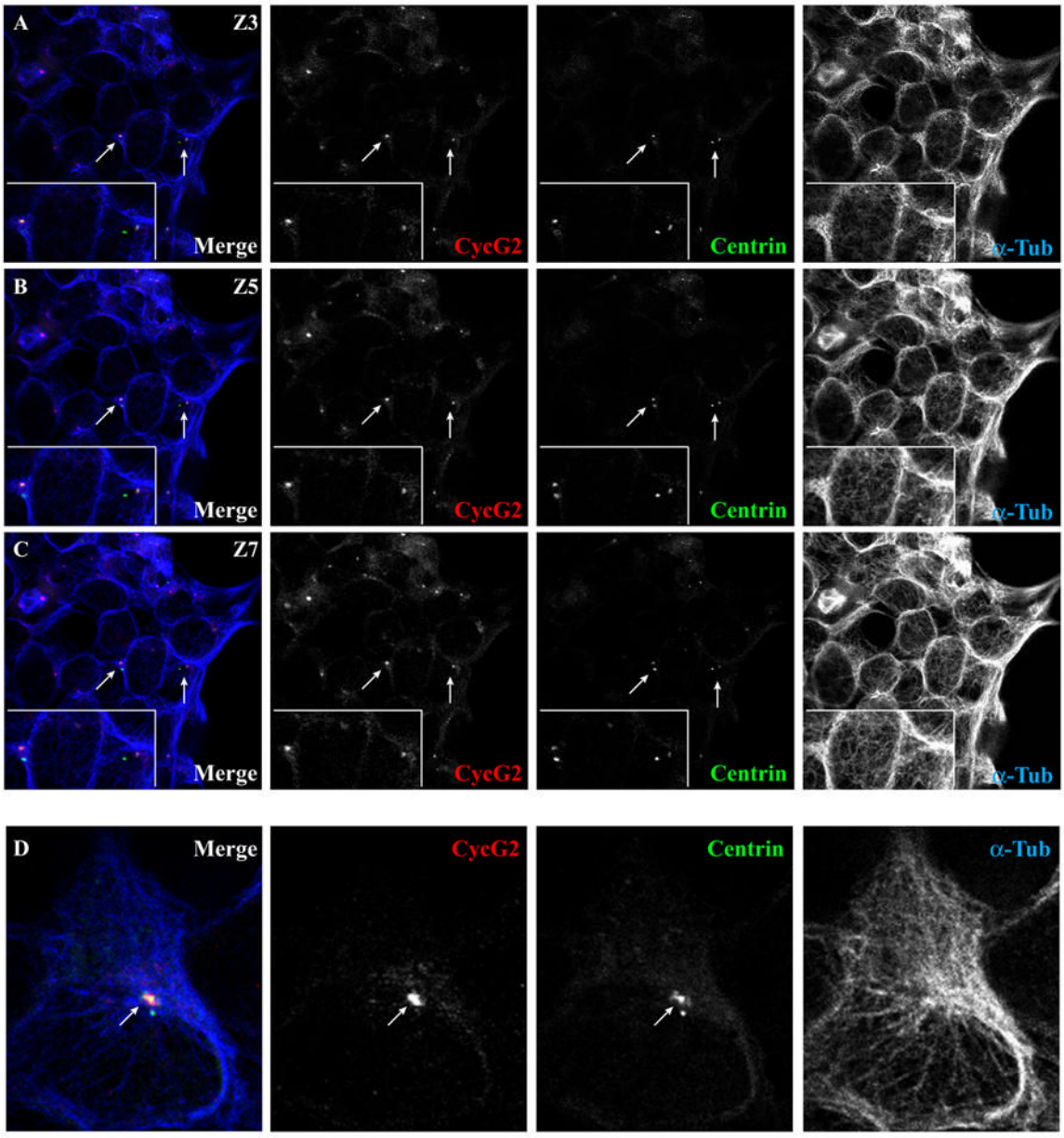

Fig. 8. Endogenous cyclin G2 localizes with only one centriole of the interphase centrosome, chiefly the MT-associated (mature) centriole

Shown are confocal immunofluorescence micrographs of U2OS cells transfected with GFP-tagged centrin and stained for endogenous cyclin G2 and α-tubulin. (A-C) Serial 0.3 μM sections (Z3, 5, and 7) of the same field show the localization of endogenous cyclin G2 staining relative to two GFP-centrin-labeled centriole pairs (arrows). The inset at the lower left shows a higher magnification of this area. Note that cyclin G2 colocalized with only one of the two GFP-centrin-positive centrioles in a pair. The cyclin G2-reactive centrioles were typically close to the center of radial MT arrays as is typical for MCs, whereas DCs are usually off this center. (D) Zoomed-in image of a GFP-centrin positive MTOC from a cell in another field showing colocalization of cyclin G2 with only one of two centrioles. Note that the larger of two GFP-labeled centrioles is at the center of a MT array and co-stained by anti-cyclin G2 antibodies,

but the smaller centriole off to the outside edge of the MTOC does not co-stain with cyclin G2 antibodies. Similar results were observed in several other independent experiments.

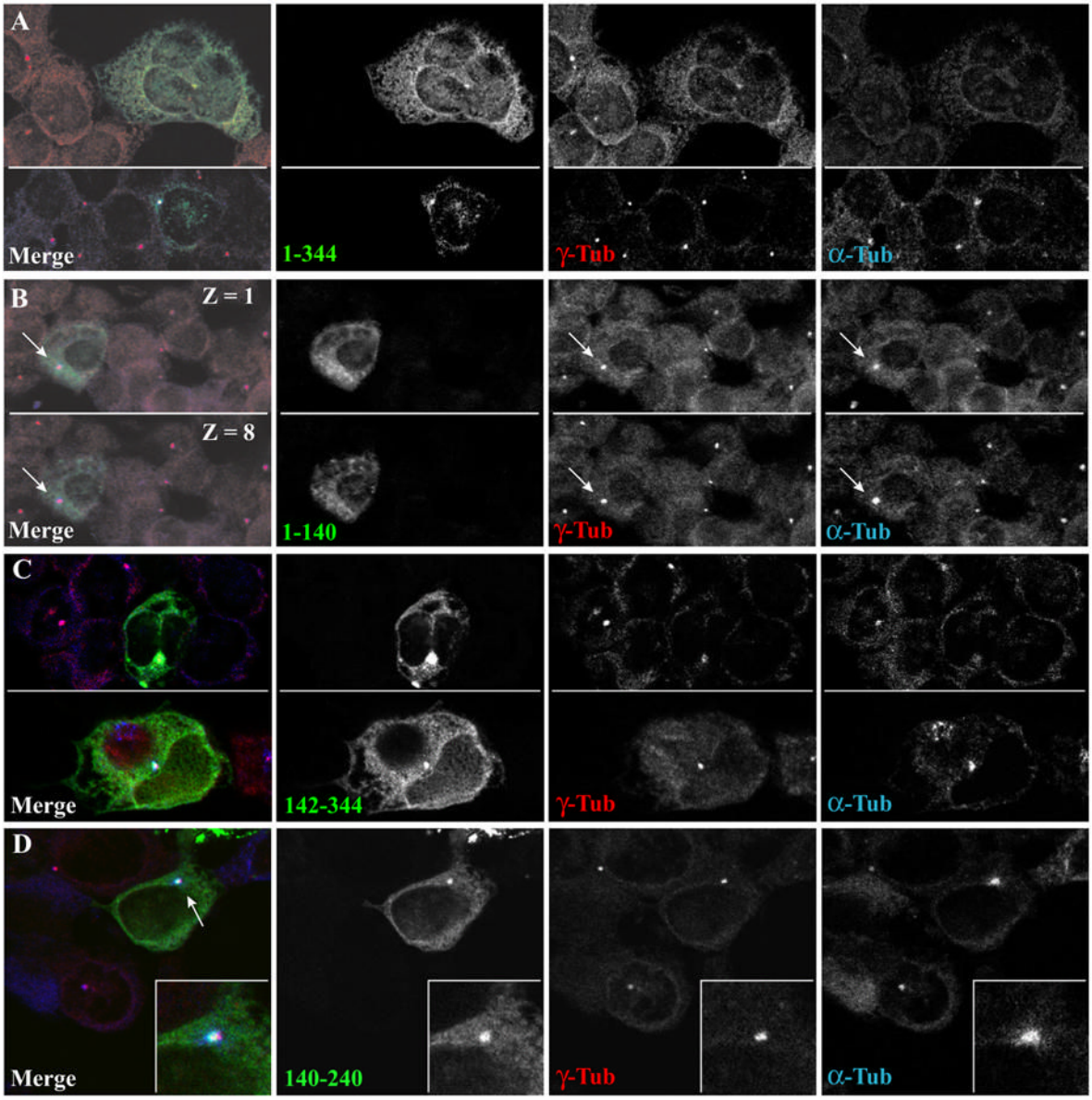

Fig. 9. The 100 amino acid carboxyterminal region of cyclin G2 that associates with PP2A directs it to the centrosome

U2OS cells transfected with constructs for the expression of GFP linked to various regions of cyclin G2, nocodazole treated, three-minute pulse released, and methanol fixed. Shown is the localization of the various cyclin G2 regions tagged with GFP relative to γ-tubulin and new bursts of MT regrowth from MTOCs. γ-tubulin and MTs (α-tubulin) were detected with the respective mouse and sheep primary antibodies as in Fig. 5B. (A) Full length cyclin G2-GFP concentrates at γ-tubulin positive MTOCs and at moderate to high levels promotes formation of multi-nuclei. (B) Top Z1 and bottom Z8 show 0.3 μM confocal sections of a cell expressing the N-terminal region of cyclin G2 spanning amino acids 1–140 fused to GFP. Note the lack of co-localization with the γ-tubulin positive MTOC. Similar to GFP alone, 1–140 GFP is largely soluble and partially extracted during MeOH fixation. (C) C-terminal cyclin G2 residues 142–344 fused to GFP concentrates to γ-tubulin positive MTOCs (top and bottom panels show two different fields of the culture). When accumulated to high levels at the

centrosome, MT regrowth is inhibited (top panel). (D) The amino acid sequence between residues 140 and 240 of cyclin G2 is sufficient to localize the corresponding GFP fusion protein to centrosomes. The inset shows a close-up of 140–240 cyclin G2-GFP colocalization with this γ-tubulin and α-tubulin positive MTOC. Similar results were obtained in several other independent experiments in U2OS, CHO, and COS-7 cells (not shown).

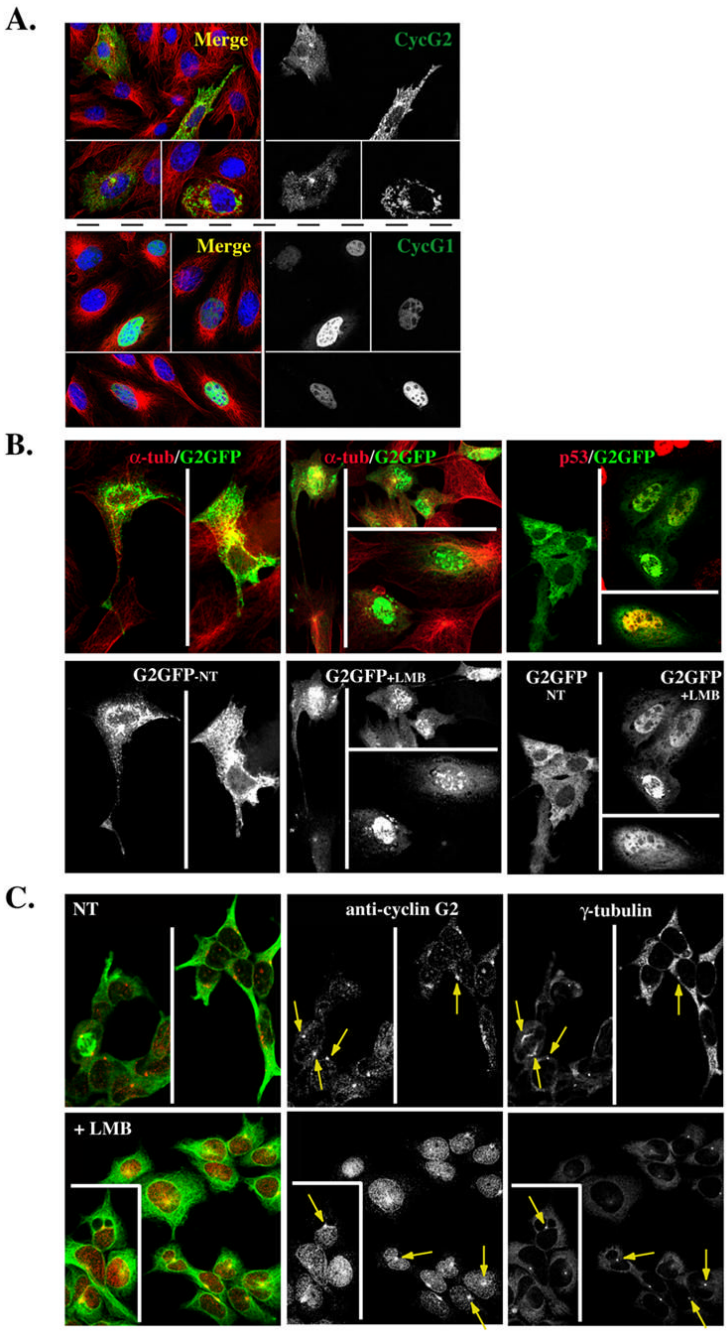

Fig. 10. Nucleocytoplasmic shuttling of G2

(A) Shown are 0.3 μM confocal immunofluorescence micrographs of NIH-3T3 cells transfected with GFP-tagged cyclin G2 (top right panel) or cyclin G1 (bottom right panel), pre-extracted with Triton X-100 and fixed with methanol. The merge to the left of each panel illustrates the corresponding G2-GFP or G1GFP co-stained for α-tubulin (green) and for DNA with TOTO-3 (blue). (B) CRM1 dependent nuclear export of ectopically expressed cyclin G2. Confocal images of G2-GFP transfected NIH3T3 cells non-treated (NT) (left panels) or LMB treated (middle panels) for 9 h, and fixed with 4% paraformaldehyde. Note the accumulation of G2-GFP in the nucleus with LMB treatment. Shown above each panel in color are corresponding merge images with DM1A mouse anti-α-tubulin (red) co-staining. Far right

panels show a repeat experiment of G2-GFP expressing cells NT (left field) or LMB treated for 9 h (right fields). The cells in the right fields were costained for p53 to confirm that the LMB treatment increases nuclear staining of a known CRM1 target protein. (C) Endogenous cyclin G2 accumulates in the nucleus of U2OS cells treated with Leptomycin B (LMB). Confocal immunofluorescence micrographs show NT (top panels) or 6 h LMB treated (bottom panels) cells, fixed in methanol, and stained for γ-tubulin, cyclin G2 and α-tubulin. The pseudo-colored image on the left shows a merge of cyclin G2 (red) and α-tubulin (green). Note the accumulation of cyclin G2 in the nucleus of LMB treated cells and yet the arrows point to the maintenance of centrosomal G2 in these treated cells.

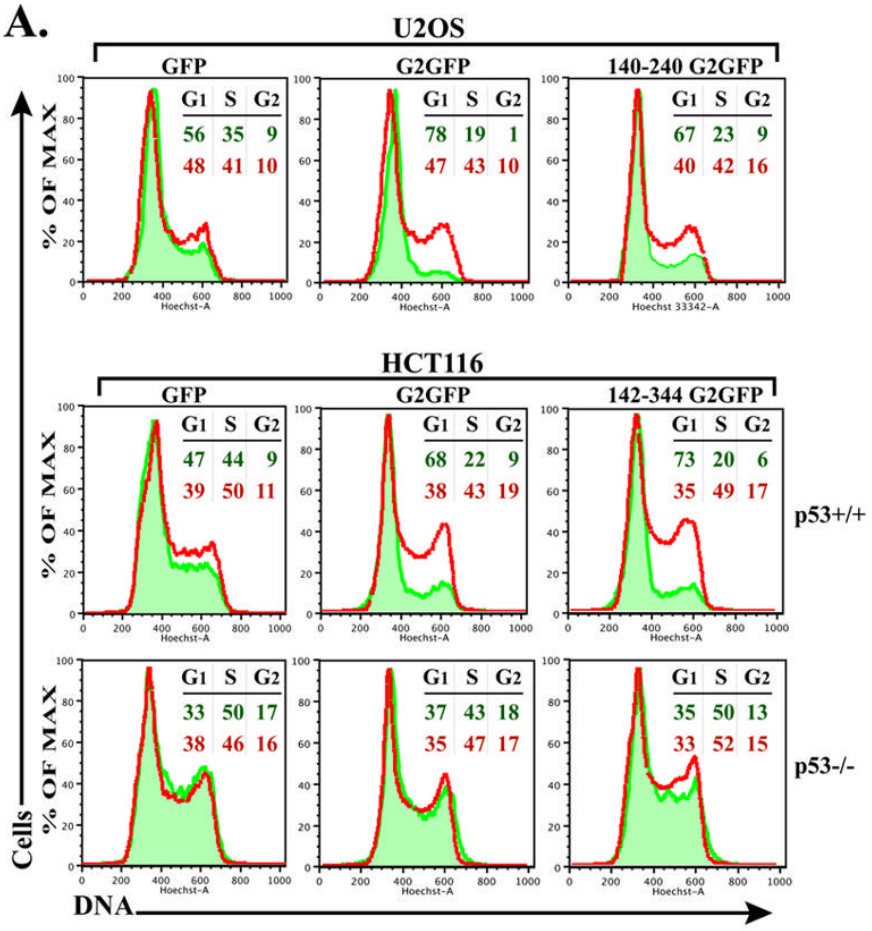

B.

Transfection		Non Expressors			Expressors		
	Cell Lines	% G1	% S	% G2	% G1	% S	% G2
G2GFP (30hrs)	p53+/+	39	42	17	64	20	14
	p53-/-	31	50	18	24	43	32
	p21-/-	32	52	16	42	30	27
GFP (30hrs)	p53+/+	27	47	26	33	43	22
	p53-/-	32	47	20	24	51	24
	p21-/-	28	54	17	27	49	24

Fig. 11. Ectopic cyclin G2 expression induces a p53-dependent cell cycle arrest that does not require p21 expression

(A) The DNA content (Hoechst 33342 labeled) of intact, (propidium iodide negative) live cells transfected with expression plasmids for full length, truncated cyclin G2-GFP, or control GFP was analyzed by flow cytometry. Amounts of DNA (Hoechst) of the GFP expressing cells are shown as histograms (shaded in green) overlaid onto the DNA histogram of the nonexpressing population (red line) from the same transfection reaction. Nonexpressing and GFP expressing cells in each transfected population were collected and analyzed simultaneously by the cytometer. The percentage of cells in the G_1, S and G_2+M phases, as determined using the FlowJo Watson Pragmatic cell cycle analysis program, is shown at the right in color-coded

font corresponding to the indicated histogram. [Similar results were obtained applying the Dean-Jett-Fox cell cycle modeling algorithm and similar results were obtained in three independent experiments for each cell line.] Top panels show analysis of U2OS cells transfected with GFP (left) full length cyclin G2-GFP (middle) and 140–240 cyclin G2-GFP (right). Middle and bottom panels illustrate the analysis of p53+/+ and p53−/− HCT116 cells, respectively, expressing GFP (left), cyclin G2-GFP (middle) and 142–344 cyclin G2-GFP (right). (B) Table shows the percentage of cells in each cell cycle phase, comparing GFP and G2-GFP expressors to nonexpressors, in p53+/+, p53−/− and p21−/− isogenic HCT116 cells as determined by the FlowJo Watson Pragmatic cell cycle analysis program. Note the intermediary effect on cell cycle arrest with ectopic expression of cyclin G2 in p21 null cells.